ScanArray – A broad band seismological experiment in the Baltic Shield

Thybo, H.[1,2], Bulut, N.[1], Grund, M.[3], Mauerberger, A.[4,5], Makushkina, A.[6], Artemieva, I.M.[7,8], Balling, N.[9], Gudmundsson, O.[10], Maupin, V.[2], Ottemøller, L.[11], Ritter, J.[3], Tilmann, F.[4,5]

[1]Eurasia Institute of Earth Sciences, Istanbul Technical University, Turkey.

[2]Center for Earth Evolution and Dynamics (CEED), University of Oslo, Norway.

[3]Karlsruhe Institute of Technology (KIT), Karlsruhe, Germany

[4] Deutsches GeoForschungsZentrum(GFZ), Potsdam, Germany

[5]Freie Universität Berlin, Berlin, Germany

[6]Australian National University, Canberra, ACT, Australia,

[7]Department of Geophysics, Stanford University, California, USA.

[8]GEOMAR Helmholtz Center for Ocean Research, Kiel, Germany

[9]Aarhus University, Aarhus, Denmark

[10]Uppsala University, Uppsala, Sweden

[11]University of Bergen, Bergen, Norway

Corresponding author:

Hans Thybo: thybo@itu.edu.tr, Eurasia Institute of Earth Sciences, Istanbul Technical University, Maslak, 34469 Istanbul, Turkey, and thybo@geo.uio.no, Center for Earth Evolution and Dynamics (CEED), University of Oslo, Blindern, 0316 Oslo, Norway

Declaration of Competing Interests

The authors acknowledge there are no conflicts of interest recorded.

ABSTRACT

The ScanArray international collaborative program has acquired broad band seismological data at 192 locations in the Baltic Shield during the period between 2012 and 2017. The main objective of the program is to provide seismological constraints on the structure of the lithospheric crust and mantle as well as the sublithospheric upper mantle. The new information will be applied to studies of how the lithospheric and deep structure affects observed fast topographic change and geological-tectonic evolution of the region. The program also provides new information on local seismicity, focal mechanisms, and seismic noise. The recordings are generally of very high quality and are used for analysis by various seismological methods, including P- and S-wave receiver functions for the crust and upper mantle, surface wave and ambient noise inversion for seismic velocity, body wave P- and S-wave tomography for upper mantle velocity structure by use of ray and finite frequency methods, and shear-wave splitting measurements for obtaining bulk anisotropy of the upper and lowermost mantle. Here we provide a short overview of the data acquisition and initial analysis of the new data, together with an example of integrated seismological results obtained by the project group along a representative ~1800 km long profile across most of the tectonic provinces in the Baltic Shield between Denmark and the North Cape. The first models support a subdivision of the Paleoproterozoic Svecofennian province into three domains, where the highest topography of the Scandes mountain range in Norway along the Atlantic Coast has developed solely in the southern and northern domains, whereas the topography is more subdued in the central domain.

INTRODUCTION

The Baltic Shield (Figure 1) is located in the northern part of Europe and includes the southern and eastern continental margins of the Arctic and North Atlantic Ocean. It was formed by amalgamation of a series of terranes and microcontinents during the Archean to the Paleoproterozoic [*Lahtinen et al.*, 2008], followed by significant modification in Neoproterozoic to Paleozoic time. The Baltic Shield includes a high mountain range, the Scandes (Figure 1a), along its western North Atlantic coast, despite being a stable craton located far from any active plate boundary. The exposed bedrock of the Baltic Shield has been subject to intensive geological mapping for more than a century and the surface geology and basement ages are known in unusual detail. The Baltic Shield therefore offers excellent conditions for studies of the relation between deep lithospheric structure and topography change as well as geological-tectonic evolution of Precambrian cratons.

The ScanArray programme made temporary deployments of broad band seismometers with a nominal spacing of 50 km in onshore Norway, Sweden and Finland during the period of 2012-2017. Two thirds of the area of the Baltic Shield had already been covered by other temporary deployments, and the 5 years long ScanArray data acquisition project completed full coverage of the remaining part of the Baltic Shield together with permanent network stations, such that high-density seismological data now exist for the whole region (Figure 2a).

A main motivation for the program is to provide uniformly distributed and consistent data for estimation of lithospheric and mantle properties of importance for ongoing studies of the mechanisms that cause topographic change in the region. The Scandes mountain range extends along the whole Scandinavian Atlantic coast with topography generally reaching above 1000 m and with a northern and a southern dome where topography exceeds 2500 m

(Figure 1a). A structurally similar mountain range exists in Greenland on the conjugate side of the North Atlantic Ocean where topography reaches above 3700 m in a ~55 Ma large volcanic zone [*Brooks*, 2011] and Jurassic sediments are observed at ~1000 m above msl [*Henriksen*, 2008], which indicates that this high topography is very young. Due to the lack of sedimentary rocks and volcanic rocks in onshore Norway it is difficult to determine the timing of the uplift, although geomorphological, fission track and other studies indicate that the high topography is recent with major uplift in the Cenozoic [*Anell et al.*, 2009; *Japsen and Chalmers*, 2000]. However, it has also been proposed that the topography has existed since the Caledonian orogeny and that the present high topography has been maintained by isostatic rebound which continuously has compensated for erosion during the last 400 My [*Nielsen et al.*, 2010]. Nevertheless, this view is seriously questioned by geological evidence [*Anell et al.*, 2010; *Gabrielsen et al.*, 2010] and the presence of sharp, high-amplitude topographic peaks around the northern dome of the Scandes.

The other main motivation for the program is to study the relation between deep lithospheric structure and geological-tectonic structure at the surface (Figure 1b). Seismic studies in the northern and eastern Baltic Shield have already revealed strong lithospheric heterogeneity *[Alinaghi et al.*, 2003; *Bruneton et al.*, 2004; *Vinnik et al., 2014; Silvennoinen et al., 2016]*, which is also expected for other parts of the shield. The complexity of the geological evolution of the region and the availability of high-quality detailed geological and seismological data makes this region an ideal laboratory for geophysical and geodynamic studies.

This paper provides an overview of the ScanArray program together with the first results based on the new data. The knowledge to be gained by the ScanArray data will be valuable for understanding the collisional tectonics that was active during the formation of the Baltic Shield, the relation between surface and deep structure, including the depth extent of thrust systems, as well as the relation between crust and mantle lithosphere in the former terranes and microcontinents that formed the Baltic Shield.

TECTONIC BACKGROUND

The Baltic Shield (Figure 1b) grew by amalgamation of a series of terranes and microcontinents onto an Archaean core in the northeast (the Kola-Karelia province) primarily during the Svecofennian orogeny from 1.9 until 1.84 Ga [*Gaal and Gorbatschev*, 1987; *Lahtinen et al.*, 2008]. *Gaal and Gorbatschev (1987)* suggest a subdivision of the Svecofennian province into three main sectors: the southern, central and northern sectors, which each represent a series of terranes and microcontinents that were amalgamated onto proto-Baltica, as later supported by seismic images [*Abramovitz et al.*, 1997; *Babel Working Group*, 1990]. Parts of the Archean core were reworked and subject to sedimentation during the Paleoproterozoic, and large parts of the Archean crust have been overthrust onto Paleoproterozoic crust as evidenced by seismic data [*Babel Working Group*, 1990; *Luosto et al.*, 1989].

The Trans-Scandinavian Igneous Belt (TIB) formed as a massive Paleoproterozoic magmatic province around the time of amalgamation of the Baltic Shield. TIB is a NNW-trending belt, which probably continues from southern Sweden below Sveconorwegian folded areas and Caledonian nappes. The subsequent ~1 Ga Sveconorwegian (Grenvillian) orogeny [*Bingen et al.*, 2008] substantially modified the outer parts of the craton and may have added terranes to present day southwestern Norway. The ~430 Ma Caledonian orogeny was caused by the collision between Baltica and Laurentia and created an 800 km wide orogenic belt along the western part of the Baltic Shield, which may have been comparable to present-day Himalaya [*Gee et al.*, 2008].

SEISMOLOGICAL BACKGROUND

The Baltic Shield has been subject to a series of temporary broad band seismological experiments since the 1990s which provided complementary data to the data stream from permanent networks (Figure 2). The low noise conditions on the exposed bedrock in most of the shield ensures acquisition of high-quality seismic data.

Earlier temporary experiments in the region include the international collaborative TOR (Tornquist Zone) project with data acquisition in 1996-97 on more than 100 stations deployed in a 100 km wide and 900 km long corridor across the SW edge of the shield into central Europe [*Gregersen et al.*, 2002; *Shomali et al.*, 2002]. This experiment demonstrated abrupt lithospheric thickening from ca. 100 km to >250 km from the southern basin area to the northern shield coinciding with strong abrupt crustal thickening from ca. 30 to 50 km [*Thybo*, 2001] as inferred from data acquired by the EUGENO-S controlled source experiment [*EUGENO-S Working Group*, 1988].

Northern and southern Sweden as well as its coastal central parts have been covered by a semi-permanent network at high density by the National Swedish Seismological Network (SNSN) since the network was substantially expanded in 2000-2008 [*SNSN*, *2004*]. Data from this national network has been applied to a series of studies of the lithospheric structure [*Eken et al.*, 2008; *Olsson et al.*, 2007]. Lithosphere seismic structure in this area is also known from controlled source seismic experiments along the ca. 2200 km long FENNOLORA controlled source profile [*Abramovitz et al.*, 2002; *Stangl*, 1990] and from the BABEL onshore-offshore project [*Abramovitz et al.*, 1997; *Babel Working Group*, 1990].

The southern dome of the Scandes was the primary target of the MAGNUS experiment in 2006-2008 with 42 stations [*Maupin et al.*, 2013; *Weidle et al.*, 2010] deployed in southern Norway and in Sweden. This broad band experiment demonstrated an abrupt transition between high-velocity lithospheric upper mantle in low-topography Sweden and low-velocity upper mantle below high-topography southern Norway, including the southern dome [*Medhus et al.*, 2012; *Wawerzinek et al.*, 2013]. It has been suggested that this difference in seismic mantle velocity may explain the high topography in the Southern Dome of the Scandes. The complementary MAGNUS REX high-frequency controlled source experiment demonstrated that the southern dome is underlain by relatively thin crust (<40 km thick) which lacks a high-velocity lower crust [*Stratford and Thybo*, 2011], and that the crust thins further across the coastline into the continental shelf [*Kvarven et al.*, 2016].

Four broad band passive source seismic profiles cross the Scandes range. The CENMOVE project deployed two approximately E-W linear arrays across the southern dome in the period of 2002-2005. [*Svenningsen et al.*, 2007] interpreted the presence of a crustal root based on receiver functions along the profiles and inferred that crustal isostasy may be the cause of the high topography. However, later controlled source profiles [*Stratford et al.*, 2009] together with areal coverage provided by receiver functions calculated from the MAGNUS data show that the Moho deepening is spatially very limited [*Frassetto and Thybo*, 2013] such that other mechanisms must be involved as cause of the high topography. These authors suggest that the absence of a high-density lower crust below the southern dome may be of importance for isostasy.

The E-W oriented broad band SCANLIPS profile provides receiver function evidence across mid-Scandinavia at ~64°N for eastward crustal thickening from the Atlantic coast to below the Central Scandes, possibly with a low velocity lower crust, which could indicate that crustal isostasy maintains the relatively shallow topography [*England and Ebbing*, 2012]. The presence of a high velocity lower crust in the Swedish part of the profile may serve to maintain the lower topography in this slightly thinner crust. Crustal thickness and structure derived from receiver functions based on the SCANLIPS2 and SCALIPS3D data around the northern dome do not indicate that crustal Airy isostasy is the cause of the very high topography here [*Ben Mansour et al.*, 2018]. However, eastward crustal thickening may also here be accompanied with the presence of a high velocity, high-density lower crust below the Fennoscandian shield, which is probably absent below the Caledonian Scandes, thereby at least partially compensating the topography through Pratt isostasy.

The SVEKALAPKO international project covered the shield in part of south-central Finland with 75 broad band and short period stations in 1998-99. Receiver functions from this experiment indicate a very deep Moho, reaching almost 65 km depth near the Archean-Proterozoic suture [*Alinaghi et al.*, 2003], which confirmed earlier observations of very thick crust based on controlled source seismic profiling [*Korsman et al.*, 1999]. Based on analysis of Rayleigh wave dispersion, [*Bruneton et al.*, 2004] infer a faster-than-average lithosphere with a thickness of at least 150 km, which is the resolution limit. Analysis of shear-wave splitting and P-wave residuals reveals spatial variation of anisotropy and lithosphere thickness across the different terranes in the study region [*Plomerova et al.*, 2006; *Vecsey et al.*, 2007].

The far northern parts of the Baltic Shield were covered by 36 broad band seismometers during the POLENET/ LAPNET experiment in 2008-2009. The data has demonstrated significant anisotropy in the lithosphere [*Vinnik et al.*, 2014] and that the lithosphere has relatively low seismic velocity and includes a significant low-velocity zone between 100 and 150 km [*Silvennoinen et al.*, 2016] . Controlled source seismic experiments show that parts of Archean Lapland have been overthrust onto younger, probably Fennoscandian, Paleoproterozoic crust [*Luosto et al.*, 1989; *Shulgin et al.*, 2018].

The data from these temporary broad band seismological deployments, complemented by controlled source seismic projects, has provided broad understanding of lithospheric and deeper structure in large parts of the Baltic Shield, but gaps in the coverage mean that this understanding was yet incomplete. The ScanArray experiment was designed to cover the remaining part such that the whole shield now has been uniformly covered by broad band seismic deployments at a station distance of 50-70 km (Figure 2a). Importantly, the new deployment covers the regions of the northern dome of the Scandes and the northern Caledonides, which were left uncovered by previous experiments. Our new seismological models will be based on the new ScanArray data together with the data from the above mentioned previous experiments.

THE ScanArray EXPERIMENT

The ScanArray experiment included the 1G Core deployment (https://www.fdsn.org/networks/detail/1G_2012) of broad band seismic stations at 72 locations in Norway, Sweden and Finland during periods of variable duration from two to five years in 2012-2017 by the universities of Copenhagen, Aarhus, Bergen and Oslo, Karlsruhe Institute of Technology (KIT), and German Research Centre for Geosciences (GFZ-Potsdam) [*Thybo et al.*, 2012] (Figure 2a, S1; Table S1; see also [*Grund et al.*, 2017] for details on the German operated stations). Additionally, University of Bergen and NORSAR deployed 28 broad band stations in the NEONOR2 array for 2½ year around the Lofoten islands in a national research program on neotectonics [*FDSN network 2D 2013-2016*]; University of Leicester deployed 20 intermediate band (60 s) stations in the dense SCANLIPS-3D array for 15 months [*England*, 2013]; and the Swedish National Seismological Network of University of Uppsala rearranged their network to complete an optimum deployment array and provided data for two years from 72 broad band (120 s) and intermediate band (30 and 60 s) stations [*SNSN*, 2004]. A list of all ScanArray related stations is provided in Table S1 and the temporal evolution of deployment is illustrated in Figure S1. The result of this deployment is that seismological data now has been acquired on stations across the whole Baltic Shield with a nominal station spacing of 50-70 km (Figure 2a), which provides unique opportunity for hitherto unfeasible comprehensive seismological studies.

The data from the ScanArray programme together with data from previous projects, supplemented by data from permanent stations, in the Baltic Shield is being interpreted by a suite of methods for studies of the lithosphere and upper mantle, local seismicity, focal mechanisms, and seismic noise. The methods applied for obtaining lithospheric structure includes P- and S-wave receiver functions for the crust and upper mantle as well as the transition zone [*Makushkina et al.*, 2019], joint surface wave – ambient noise tomography for seismic velocity [*Mauerberger et al.*, 2020], beam-forming surface wave analysis [*Mauerberger et al., in prep.*], body wave P- and S- wave tomography for upper mantle velocity structure by use of ray and finite frequency methods [*Bulut et al., in prep., Lutz et al., in prep.]*, and shear-wave splitting measurements (using SKS, SKKS, PKS, and sSKS phases) for obtaining bulk anisotropy of the upper and lowermost mantle [*Grund and Ritter*, 2019; *Grund and Ritter*, 2020].

Because of the uneven duration of deployment of the seismic stations, the number of useful events for application of the various methods varies. Deployment for very long periods of 4-5 years of 39 stations from Denmark, together with a large number of permanent stations, presents unique opportunity for interpretation of anisotropy by beam-forming analysis of teleseismic records at high accuracy [*Mauerberger et al.*, 2020]. Furthermore, favored by its large-aperture geometry and its nearly perfect location with respect to the epicentral distance from earthquake sources to the ScanArray receivers, the network enabled studies of anisotropy in so far unexplored regions in the D'' layer (~ 2700 km depth) beneath the Atlantic Ocean and Siberia[*Grund and Ritter*, 2019]. Finite frequency tomography could make use of 634 and 404 events for reading of direct P- and S-wave traveltimes, respectively. The event distribution (Figure 2b) is biased towards arrivals from earthquakes in the western Pacific subduction system at back-azimuths between 0° and 100° with a clear concentration around 50° corresponding to events in Japan, and a low number of useful events with southerly back-azimuths between 150° and 270°.

In general, most of the stations provide data of high quality in a frequency range appropriate for all kinds of regional tomographic and receiver function studies, although the noise level varies with geographical location, in particular regarding the cultural and ocean noise. Figure 3 illustrates the noise level in the network with power spectral density plots for the vertical (Z) and North-South (N) components of three stations. We omit the East-West components since they show the same level of noise as the North-South components. Station N2HS (68.1033N and 15.5137E, Nordland region of Norway) is a coastal station that was part of the NEONOR2 deployment. Station SA20 (66.4298N, 19.6862E) is located in northern Sweden and station SA39 (64.0718, 14.0906E) in central Sweden close to the Norwegian border. Station SA20 is one of the high-noise-level stations reaching nearly the New High Noise Model curve (Peterson, 1993), whereas station SA39 is a typical example with a relatively low noise level across the entire period range in the middle between the New High and New Low Noise Models after Peterson (1993). The majority of stations were installed indoors, which results in slightly higher noise levels at both short ($T < 0.2$ s) and long periods ($T > 10$ s) than for permanent network stations (e.g., Demuth et al., 2017; Ottemöller et al., 2020). Noise levels are variable due to individual site conditions and station configurations. The short period noise depends mostly on the distance to cultural noise sources. The noise at periods 0.2-1 s partly reflects the weather conditions and generally decreases away from the coast. Longer period ocean noise is, however, present far inland and is the aim of on-going ambient noise studies. Power spectral density plots for the stations belonging to the Geophysical Instrument Pool Potsdam, located mostly around the Bothnian Bay in Sweden and Finland, can be found in Grund et al. (2017). They show a level of noise similar to the one presented in Figure 3.

We also present two waveform examples from a regional and a teleseismic earthquake to demonstrate the overall quality of the new recordings: (1) The local March 19, 2016 magnitude 4.1 strike-slip earthquake event in the Bothnian Bay from which the seismic phases are clearly visible across the complete ScanArray network (Fig. 4a); and (2) The teleseismic magnitude 7.8 thrust faulting event from Khudi, Nepal on April 25, 2015 (Fig. 4b).

EXAMPLE RESULTS

The interpretation of the new seismic data is well underway. We illustrate the results with an integrated profile across the whole Baltic Shield from south to north (Figure 1). The profile (Fig. 5a) shows modest topographic variation between 0 and ~700 m above mean sea level. It crosses from south to north (Fig. 1b) a narrow zone covered with Phanerozoic sedimentary rocks (1, Sed), the Sveconorwegian zone (2, SN), the Trans-Scandinavian Igneous Belt (3, TIB), the southern, central and northern Svecofennian provinces (4, SSF; 5, CSF; 6, NSF), the reworked Archean zone (7, Archean) which may have been overthrust onto Proterozoic lithosphere, and into the zone affected by the Caledonian orogeny (8, Cal). This profile does not cross the areas with the highest topography in Fennoscandia; interpretation of these areas will be presented in a series of specialized papers.

The seismological interpretations show significant structural variability along the profile, and the applied methods each provide complementary information about structure and properties of the crust and upper mantle. Resolution varies for the methods applied, where receiver function results generally have high vertical resolution of discontinuities, models based on surface wave analysis have relatively high vertical and lower horizontal resolution, and models based on body wave traveltime inversion and shear-wave splitting analysis have low vertical resolution and higher horizontal resolution determined by station density. The

ScanArray experiment has provided two main improvements to the knowledge of the seismic structure of the Fennoscandian lithospheric mantle: (1) The whole region has now been covered by broad band seismological data acquisition at approximately the same station coverage of nominally 50 km spacing which ensures areal coverage of the seismic models, and (2) Several of the ScanArray (1G) stations were operating for 4-5 years, which provides new opportunity for detailed studies of, in particular, anisotropy at high resolution.

Joint surface wave and ambient noise tomography (Fig. 5b), in the following referred to as surface wave tomography, shows some heterogeneity within the crust and surprisingly large variability in velocity around the Moho, where low seismic velocities around the Moho may represent underplated material [*Thybo and Artemieva*, 2013] emplaced during the amalgamation of the shield and formation of TIB or alternatively, but less likely, the presence of metamorphosed rocks in the form of e.g. serpentinite. The P- and S-wave receiver functions (Fig. 5c,d) show large variation in crustal thickness from about 35 to 50 km along the profile, and the S-wave receiver functions appear to show double converters at suggested underplated zones. The surface wave tomography S-wave velocity model of the upper mantle shows large variability with the highest shear-wave velocities (Vs) in the Svecofennian terranes, whereas the Archaean and Sveconorwegian zones generally have lower velocity [*Mauerberger et al.*, 2020]. The preliminary body wave tomography shows comparable P- and S-wave velocity (Vp and Vs) structure (Fig. 5f,g) along most of the profile with the highest seismic velocities in the lithospheric mantle velocities observed in the Svecofennian terranes. The variable Vp/Vs anomalies (Fig. 5h) indicate substantial compositional variation along the profile. P-wave receiver functions (Fig. 5i) targeting the mantle transition zone reveal that the transition zone has constant thickness throughout the Baltic Shield, from which *Makushkina et al. (2019)* infer that the high topography in the Scandes cannot be caused by a deeply seated thermal anomaly because, otherwise, the thickness of the transition zone would be affected. The ‘410’ and ‘660’ discontinuities appear to be generally shallower than expected which probably reflects an artifact associated with the depth conversion since the seismic velocities in the Baltic Shield are higher than the global average. The mantle P-wave receiver functions exhibit strong signals in the 100-200 km depth interval, which may represent multiples, although parts of this signal probably can be attributed [*Makushkina et al.*, 2019] to a Mid Lithospheric Discontinuity (MLD, cf. [*Abt et al.*, 2010; *Perchuc and Thybo*, 1996] and the underlying low-velocity zone [*Thybo*, 2006]. Seismic anisotropy (Fig. 5j) from studies of shear-wave splitting for various core-refracted phases [*Grund and Ritter*, 2020] demonstrates large variability along the profile with clear correlation between changes in anisotropy and the main tectonic zones.

The main tectonic zones exhibit individual lithospheric properties. The sediment covered region at the southern edge of the profile (marked 1 and Sed) has low upper crustal and high lower-crustal Vs (Fig. 5b), which may be explained by a thick sedimentary cover above a large crustal intrusion [*Thybo*, 2001]. It appears to have very low Vp and Vs from the Moho to depths of at least 200 km (Fig. 5b,e,f,g), in accordance with earlier body-wave tomography along the TOR profile [*Shomali et al.*, 2002]. The low uppermost mantle velocities coincide with a zone of small Vp/Vs ratio (Fig. 5h) which indicates compositional heterogeneity compared to undisturbed upper mantle zones.

The Sveconorwegian affected zone (SN) includes a part with low sub-Moho Vs, extending from the sediment covered part, which may be indicative of underplated material, as also supported by the very high Vp/Vs ratio that extends deep into the upper mantle. S-wave receiver functions show two converters, one at the Moho and the other at deeper level, around the depth interval of the low velocity zone, which may add support to the presence of underplated material. The Sveconorwegian zone shows distinct, strong anisotropy with fast axes oriented differently from the surrounding zones. With the data from the BABEL controlled source reflection and refraction experiment, this zone was identified as a hidden crustal terrane with its own specific P-wave velocity structure of the crust and uppermost mantle, including a highly reflective lower crust, which was interpreted to result from anastomosing shear zones in mafic or fluid rich lowermost crust. However, the Pn velocity was normal for a shield area {*Abramovitz et al., 1997*].

The Trans Scandinavian Igneous Belt (TIB) includes a distinct thin low-velocity body below the Moho, which coincides with a double set of S-wave receiver function converters. Here there is a tendency that the P-wave receiver functions also show a double converter. However, the mantle velocities from ~60 to ~150 km depth are high with low Vp/Vs ratio. Moderate anisotropy is observed with an EW directed fast axis, which differs from the surrounding zones.

The Svecofennian domains all have high Vp and Vs in the upper mantle with distinctly different Vp/Vs ratio and distinctly different anisotropy between the three domains along the profile, which provides support for the division into the domains proposed by [*Gaal and Gorbatschev*, 1987]. The receiver function conversion from the ‘660’ is generally strong along the whole profile, whereas the ‘410’ conversion loses amplitude in the central Svecofennian domain. High Vp and Vs are observed in the southern province (SSF) below a single converter Moho. The sub-Moho Vs is remarkably low in a 20 km thick zone within the central Svecofennian domain. This low velocity layer appears bounded by very strong individual S-wave receiver function converters throughout the domain. The highest upper mantle velocities and high Vp/Vs ratio are observed in the Central Svecofennian domain in a layered internal structure. Remarkably, the receiver function arrivals in the 100-200 km depth interval appear disrupted across the central domain, which may be explained by weak multiples due to low contrast between a fast lower crust and an intermediate velocity mantle directly beneath the Moho. The northern Svecofennian province is characterized by a strong, sharp Moho conversion in both P- and S-wave receiver function stacks, which also shows up as a strong gradient in the surface wave tomography. Nevertheless, the S-wave receiver function again indicates the presence of another converter in the upper mantle. The shear-wave splitting model by *Grund and Ritter [2020]* favors a NE dipping anisotropic layer that may be related to Proterozoic northwards subduction (Fig. 5j), as earlier observed at the southern edge of this northern domain from controlled source seismic data [*Babel Working Group*, 1990].

The results from the reworked Archean area largely resemble the results from the northern Svecofennian domain in all parameters, which supports the interpretation that a thin Archean upper crustal layer generally is overlying Paleaoproterozoic lithosphere in this area. However, the observed anisotropy is distinctly different from the northern Svecofennian domain, which may indicate different directions of plate movement during the evolution. The 100 km wide corridor in the Caledonian deformed domain generally show results similar to the neighboring domain, which indicates that the influence of the Caledonian orogeny here only had limited effect on the deep crustal and mantle lithosphere structure.

It is remarkable that the two domes of the Scandes occur in the southern and northern Svecofennian domains only (Fig. 5k). Although our example profile does not directly cross these domes, we notice that these domains have relatively lower velocity than the central domain according to both the surface and body wave tomography and that only the central domain of the Svecofennian province show low sub-Moho Vs as indication for very thick underplating. The anisotropy parameters in the southern and northern domains are also comparable and distinctly different from the central domain (Fig. 5j). The illustrated profile crosses parts of Fennoscandia with very limited topography, which gradually increases from sea level in the south to ~500 m in the Archean domain in the far north. However, none of the new images show correlation to this gradual change in topography, and one may speculate that the changes in physical parameters required for the modest topographic variations are too subtle to be imaged within the resolution obtained with the seismological methods applied. The S-wave receiver function profile (Fig. 5d) may show some correlation with the topography. It shows generally two positive converters, which are very close in the south and more than 20 km apart to the north of 62ºN where the topography is higher than 300 m. We find that the profile indicates that our seismological results cannot constrain subtle, long-wavelength changes in topography of less than up to 500 m.

CONCLUSIONS

The data acquisition by the ScanArray consortium has ensured that the whole Baltic Shield, including the Caledonian deformed crust, now has been fully covered by broad band, passive seismic data at high quality. A series of significant seismological results are already published and results from a variety of other studies are underway.

We demonstrate significantly different seismological properties between eight tectonic segments along a N-S trending profile across the whole Baltic Shield. The velocity model shows strong variation around the Moho along the profile, where intermediate velocities between crust and mantle tend to correlate with the presence of two receiver function converters, possibly representing underplated regions. The lithospheric mantle in the Svecofennian parts of the region has higher velocity than in both the Archean and younger (Sveconorwegian and Caledonian) parts, although the Vp/Vs ratio varies within each of these parts. While the resolution of our seismological methods may be insufficient to identify causes for subtle, long-wavelength changes in topography, our results show that the high topography in the two domes of the Scandes mountain range has developed in two distinct domains of the Svecofennian province of the Baltic Shield which are characterized by significantly different seismic parameters in the crust and upper mantle than the surrounding areas with less topography.

DATA AND RESOURCES

Most data from the ScanArray Core data set has been publicly available since 1 January 2021 within EIDA from the GEOFON data center (FSDN network code 1G2012-2017, doi:10.14470/6T569239). The remaining data from stations operating until September 2017 will become publicly available from the same site by September 2021. Data from UiB are available from https://doi.org/10.7914/SN/NS (University of Bergen, 1982); from NORSAR at doi: 10.21348/d.no.0001 (NORSAR, 1971); and from Helsinki from https://doi.org/10.14470/UR044600 Institute of Seismology, University of Helsinki, 1980). Data from the Northern Finland network is available at https://www.fdsn.org/networks/detail/FN. Supplementary Material includes details of the deployment program in Figure S1 and Table S1. Figures were partly prepared using Generic Mapping Tools (GMT and PyGMT, *Wessel et al.*, 2019; *Uieda et al., 2021*).

ACKNOWLEDGMENTS

The authors are grateful for insightful reviews by Richard England and Myrto Pirli. The ScanArray data acquisition has been supported by grants from Danish Council for Independent Research (Grant Nos. FNU16-059776-15 to H. Thybo and DFF-1323-00053 to I.M. Artemieva), and Istanbul Technical University (grant No. BAPSIS TGA-2019-41593 to H. Thybo). V. Maupin and H. Thybo acknowledge support from the Department of Geosciences of the University of Oslo and the Research Council of Norway through its Centers of Excellence funding scheme, Project Number 223272, to Center for Earth Evolution and Dynamics. Support is acknowledged from the Carlsberg Foundation (grant 2013_01_0337 to N. Balling and grant 2012_01_0396 to H. Thybo), and the German Research Foundation (project LITHOS-CAPP, grants TI 316/3-1, -2 to F. Tilmann and RI1133/11-1, -2 to J. Ritter). Field work in Finland was kindly supported by E. Kozlovskaya and H. Silvennoinen (University of Oulu). Seismic instruments for the German contribution to ScanArray were kindly provided by the Geophysical Instrument Pool Potsdam at GFZ Potsdam. We thank Felix Halpaap (Univ. of Bergen) for providing the PSDPDFs of Figure 3.

REFERENCES

Abramovitz, T., A. Berthelsen, and H. Thybo (1997), Proterozoic sutures and terranes in the southeastern Baltic Shield interpreted from BABEL deep seismic data, *Tectonophysics*, *270*, 259-277, doi:10.1016/s0040-1951(96)00213-2.

Abramovitz, T., H. Thybo, and E. Perchuc (2002), Tomographic inversion of seismic P- and S-wave velocities from the Baltic Shield based on FENNOLORA data, *Tectonophysics*, *358*, 151-174.

Abt, D. L., K. M. Fischer, S. W. French, H. A. Ford, H. Y. Yuan, and B. Romanowicz (2010), North American lithospheric discontinuity structure imaged by Ps and Sp receiver functions, *J. Geophys. Res.*, *115*, doi:10.1029/2009jb006914.

Alinaghi, A., et al. (2003), Receiver function analysis of the crust and upper mantle from the North German Basin to the Archaean Baltic Shield, *Geophys. J. Int.*, *155*, 641-652, doi:10.1046/j.1365-246X.2003.02075.x.

Anell, I., H. Thybo, and I. M. Artemieva (2009), Cenozoic uplift and subsidence in the North Atlantic region: Geological evidence revisited, *Tectonophysics*, *474*, 78-105.

Anell, I., H. Thybo, and W. Stratford (2010), Relating Cenozoic North Sea sediments to topography in southern Norway: The interplay between tectonics and climate, *Earth and Planetary Science Letters*, *300*(1-2), 19-32, doi:10.1016/j.epsl.2010.09.009.

BABEL Working Group (1990), Evidence for early Proterozoic plate tectonics from seismic reflection profiles in the Baltic Shield, *Nature*, *348*, 34-38.

Ben Mansour, W., R. W. England, S. Fishwick, and M. Moorkamp (2018), Crustal properties of the northern Scandinavian mountains and Fennoscandian shield from analysis of teleseismic receiver functions, *Geophys. J. Int.*, *214*, 386-401, doi:10.1093/gji/ggy140.

Bingen, B., J. Andersson, U. Soderlund, and C. Moller (2008), The Mesoproterozoic in the Nordic countries, *Episodes*, *31*, 29-34, doi:10.18814/epiiugs/2008/v31i1/005.

Brooks, C. K. (2011), The East Greenland rifted volcanic margin, *Geol. Surv. Denmark Greenland Bull.*, *24*, 96 pp.

Bruneton, M., et al. (2004), Complex lithospheric structure under the central Baltic Shield from surface wave tomography, *J. Geophys. Res.*, *109*, *doi*: 10.1029/2003JB002947.

Casey R., Templeton M. E., Sharer G., Keyson L., Weertman B. R., and Ahern T. (2018), Assuring the quality of IRIS data with MUSTANG, *Seismol. Res. Lett. 89, no. 2A, 630–639*.

Demuth, A., Ottemoller, L and Keers, H., (2016). Ambient noise levels and detection threshold in Norway, *J. Seismol. 20, 889-904*.

Eken, T., Z. H. Shomali, R. Roberts, C. F. Hieronymus, and R. Bodvarsson (2008), S and P velocity heterogeneities within the upper mantle below the Baltic Shield, *Tectonophysics*, *462*(1-4), 109-124, doi:10.1016/j.tecto.2008.02.015.

England, R. (2013), SCANLIPS3D [Data set], edited, International Federation of Digital Seismograph Networks, https://doi.org/10.7914/SN/ZR_2013.

England, R. W., and J. Ebbing (2012), Crustal structure of central Norway and Sweden from integrated modelling of teleseismic receiver functions and the gravity anomaly, *Geophys. J. Int.*, *191*, 1-11, doi:10.1111/j.1365-246X.2012.05607.x.

EUGENO-S Working Group (1988), Crustal structure and tectonic evolution of the transition between the Baltic Shield and the North German Caledonides (the EUGENO-S project), *Tectonophysics*, *150*, 253-348.

Frassetto, A., and H. Thybo (2013), Receiver function analysis of the crust and upper mantle in Fennoscandia - isostatic implications, *Earth Plan. Sci. Lett.*, *381*, 234-246, doi:10.1016/j.epsl.2013.07.001.

Gaal, G., and R. Gorbatschev (1987), An outline of the Precambrian evolution of the Baltic Shield, *Precam. Res.*, *35*, 15-52, doi:10.1016/0301-9268(87)90044-1.

Gabrielsen, R. H., J. I. Faleide, C. Pascal, A. Braathen, J. P. Nystuen, B. Etzelmuller, and S. O'Donnell (2010), Latest Caledonian to Present tectonomorphological development of southern Norway, *Mar. Petr. Geol.*, *27*, 709-723, doi:710.1016/j.marpetgeo.2009.1006.1004.

Gee, D. G., H. Fossen, N. Henriksen, and A. K. Higgins (2008), From the early Paleozoic platforms of Baltica and Laurentia to the Caledonide orogen of Scandinavia and Greenland, *Episodes*, *31*, 44-51.

Gregersen, S., et al. (2002), Summary of project TOR: delineation of a stepwise, sharp, deep lithosphere transition across Germany-Denmark-Sweden, *Tectonophysics*, *360*, 61-73, doi:10.1016/s0040-1951(02)00347-5.

Grund, M., A. Mauerberger, J. Ritter, and F. Tilmann (2017), Broadband Recordings for LITHOS-CAPP: LITHOspheric Structure of Caledonian, Archaean and Proterozoic Provinces , Sep. 2014 - Oct. 2016, Sweden and Finland, edited, Tech. rep, doi:10.2312/GFZ.b103-17029.

Grund, M., and J. R. R. Ritter (2019), Widespread seismic anisotropy in Earth's lowermost mantle beneath the Atlantic and Siberia, *Geology*, *47*, 123-126, doi:10.1130/g45514.1.

Grund, M., and J. R. R. Ritter (2020), Shear-wave splitting beneath Fennoscandia — evidence for dipping structures and laterally varying multilayer anisotropy, *Geophys. J. Int.*, *223*, 1525-1547, doi:10.1093/gji/ggaa388.

Henriksen, N. E. (2008), Geological History of Greenland - Four billion years of Earth evolution, *Geological Survey of Denmark and Greenland*, 272pp.

Institute of Seismology, University of Helsinki (1980): The Finnish National Seismic Network. Deutsches GeoForschungsZentrum GFZ. Other/Seismic Network. doi:10.14470/UR044600.

Japsen, P., and J. A. Chalmers (2000), Neogene uplift and tectonics around the North Atlantic: overview, *Global and Planetary Change*, *24*, 165-173.

Korsman, K., et al. (1999), The GGT/SVEKA transect: Structure and evolution of the continental crust in the Paleoproterozoic Svecofennian orogen in Finland, *Int. Geol. Rev.*, *41*, 287-333.

Kvarven, T., R. Mjelde, B. O. Hjelstuen, J. I. Faleide, H. Thybo, E. R. Flueh, and Y. Murai (2016), Crustal composition of the Møre Margin and compilation of a conjugate Atlantic margin transect, *Tectonophysics*, *666*, doi:https://doi.org/10.1016/j.tecto.2015.11.002.

Lahtinen, R., A. A. Garde, and V. A. Melezhik (2008), Paleoproterozoic evolution of Fennoscandia and Greenland, *Episodes*, *31*, 20-28, doi:10.18814/epiiugs/2008/v31i1/004.

Luosto, U., E. R. Flueh, and C. E. Lund (1989), The crustal structure along the POLAR profile from seismic refraction investigations, *Tectonophysics*, *162*, 51-85, doi:10.1016/0040-1951(89)90356-9.

Makushkina, A., B. Tauzin, H. Tkalčić, and H. Thybo (2019), The mantle transition zone in Fennoscandia: Enigmatic high topography without deep mantle thermal anomaly, *Geophys. Res. Lett.*, *46*, doi:10.1029/2018GL081742.

Mauerberger, A., V. Maupin, Ó. Gudmundsson, and F. Tilmann (2020), Anomalous azimuthal variations with 360° periodicity of Rayleigh phase velocities observed in Scandinavia, *Geophys. J. Int.*, *224*, 1684-1704, doi:10.1093/gji/ggaa553.

Maupin, V., et al. (2013), The deep structure of the Scandes and its relation to tectonic history and present-day topography, *Tectonophysics*, *602*, 15–37, doi:http://dx.doi.org/10.1016/j.tecto.2013.03.010.

Medhus, A. B., N. Balling, B. H. Jacobsen, C. Weidle, R. W. England, R. Kind, H. Thybo, and P. Voss (2012), Upper-mantle structure beneath the Southern Scandes Mountains and the Northern Tornquist Zone revealed by P-wave traveltime tomography, *Geophys. J. Int.*, *189*, 1315-1334, doi:10.1111/j.1365-246X.2012.05449.x.

Nielsen, S. B., O. R. Clausen, B. H. Jacobsen, E. Thomsen, M. Huuse, K. Gallagher, N. Balling, and D. Egholm (2010), The ICE hypothesis stands: How the dogma of late Cenozoic tectonic uplift can no longer be sustained in the light of data and physical laws, *J. Geodyn.*, *50*, 102-111, doi:10.1016/j.jog.2010.02.002.

NORSAR (1971). NORSAR Station Network [Data set], https://doi.org/10.21348/d.no.0001

Olsson, S., R. G. Roberts, and R. Boovarsson (2007), Analysis of waves converted from S to P in the upper mantle beneath the Baltic Shield, *Earth Plan. Sci. Lett.*, *257*(1-2), 37-46, doi:10.1016/j.epsl.2007.02.017.

Ottemöller, L., Michalek, J., Christensen, J-M., Baadshaug U., Halpaap F., Natvik, Ø., Kværna, T. and Oye V. (2021). UiBNORSAR EIDA Node: Integration of Seismological Data in Norway, *Seismol. Res. Lett.* XX, 1–10, doi: 10.1785/0220200369.

Perchuc, E., and H. Thybo (1996), A new model of upper mantle P-wave velocity below the Baltic Shield: Indication of partial melt in the 95 to 160 km depth range, *Tectonophysics*, *253*, 227-245, doi:10.1016/0040-1951(95)00057-7.

Peterson, J. (1993), Observations and Modeling of Seismic Background Noise, *U.S. Geological Survey Open-File report* 93-322, Albuquerque, N.M.

Plomerova, J., V. Babuska, L. Vecsey, E. Kozlovskaya, T. Raita, and Sstwg (2006), Proterozoic-Archean boundary in the mantle lithosphere of eastern Fennoscandia as seen by seismic anisotropy, *J. Geodyn.*, *41*, 400-410, doi:10.1016/j.jog.2005.10.008.

Shomali, Z. H., et al. (2002), Non-linear body wave teleseismic tomography along the TOR array, *Geophys. J. Int.*, *148*, 562-574, doi:10.1046/j.1365-246x.2002.01592.x.

Shulgin, A., R. Mjelde, J. I. Faleide, T. Høy, E. Flueh, and H. Thybo (2018), The crustal structure in the transition zone between the western and eastern Barents Sea, *Geophys. J. Int.*, *214*, 315-330, doi:https://doi.org/10.1093/gji/ggy139.

Silvennoinen, H., E. Kozlovskaya, and E. Kissling (2016), POLENET/LAPNET teleseismic P wave travel time tomography model of the upper mantle beneath northern Fennoscandia, *Solid Earth*, *7*, 425-439, doi:10.5194/se-7-425-2016.

SNSN (2004), Seismic network. doi:10.18159/SNSN, edited, Uppsala University, Uppsala, Sweden.

Stangl, R. (1990), Die Struktur der Lithosphäire in Schweden, abgeleitet aus einer gemeinsamen Interpretation der P- und S-Wellen Registrierungen auf dem FENNOLORA-Profil., PhD thesis, 187 pp., *University of Karlsruhe*.

Stratford, W., and H. Thybo (2011), Seismic structure and composition of the crust beneath the southern Scandes, Norway, *Tectonophysics*, *502*, 364-382, doi:https://doi.org/10.1016/j.tecto.2011.02.008.

Stratford, W., H. Thybo, J. I. Faleide, O. Olesen, and A. Tryggvason (2009), New Moho Map for onshore southern Norway, *Geophys. J. Int.*, *178*(3), 1755-1765.

Svenningsen, L., N. Balling, B. H. Jacobsen, R. Kind, K. Wylegalla, and J. Schweitzer (2007), Crustal root beneath the highlands of southern Norway resolved by teleseismic receiver functions, *Geophys. J. Int.*, *170*, 1129-1138.

Thybo, H. (2001), Crustal structure along the EGT profile across the Tornquist Fan interpreted from seismic, gravity and magnetic data, *Tectonophysics*, *334*, 155-190.

Thybo, H. (2006), The heterogeneous upper mantle low velocity zone, *Tectonophysics*, *416*, 53-79.

Thybo, H., and I. M. Artemieva (2013), Moho and magmatic underplating in continental lithosphere, *Tectonophysics*, *609*, 605-619, doi:http://dx.doi.org/10.1016/j.tecto.2013.05.032.

Thybo, H., N. Balling, V. Maupin, J. R. R. Ritter, and F. Tilmann (2012), ScanArray Core (1G 2012-2017), edited, The ScanArray consortium, GEOFON database, doi:10.14470/6T569239.

University Of Bergen. (1982). *University of Bergen Seismic Network* [Data set]. International Federation of Digital Seismograph Networks. https://doi.org/10.7914/SN/NS

Uieda, L., D. Tian, W.J. Leong, L. Toney, W. Schlitzer, M. Grund, T. Newton, M. Ziebarth, and P. Wessel (2021), PyGMT: A Python interface for the Generic Mapping Tools, v0.3.0, Zenodo, doi:10.5281/zenodo.4522136.

Vecsey, L., J. Plomerova, E. Kozlovskaya, and V. Babuska (2007), Shear wave splitting as a diagnostic of variable anisotropic structure of the upper mantle beneath central Fennoscandia, *Tectonophysics*, *438*, 57-77, doi:10.1016/j.tecto.2007.02.017.

Vinnik, L., et al. (2014), Anisotropic lithosphere under the Fennoscandian shield from P receiver functions and SKS waveforms of the POLENET/LAPNET array, *Tectonophysics*, *628*, 45-54, doi:10.1016/j.tecto.2014.04.024.

Wawerzinek, B., J. R. R. Ritter, and C. Roy (2013), New constraints on the 3D shear wave velocity structure of the upper mantle underneath Southern Scandinavia revealed from non-linear tomography, *Tectonophysics*, *602*, 38-54, doi:10.1016/j.tecto.2012.12.033.

Weidle, C., V. Maupin, J. Ritter, T. Kvaerna, J. Schweitzer, N. Balling, H. Thybo, J. I. Faleide, and F. Wenzel (2010), MAGNUS—A Seismological Broadband Experiment to Resolve Crustal and Upper Mantle Structure beneath the Southern Scandes Mountains in Norway, *Seis. Res. Lett.*, *81*, 76-84, doi:10.1785/gssrl.81.1.76.

Wessel, P., J.F. Luis, L. Uieda, R. Scharroo, F. Wobbe, W.H.F. Smith, and D. Tian (2019), The Generic Mapping Tools version 6, *Geochem.,Geophys., Geosys.*, 20, 5556–5564, doi: 10.1029/2019GC008515.

MAILING ADDRESSES

Thybo, H.: thybo@itu.edu.tr, Eurasia Institute of Earth Sciences, Istanbul Technical University, Maslak, 34469 Istanbul, Turkey, and Center for Earth Evolution and Dynamics (CEED), University of Oslo, Blindern, 0316 Oslo, Norway

Bulut, N.: nevra.bulut@gmail.com, Eurasia Institute of Earth Sciences, Istanbul Technical University, Maslak, 34469 Istanbul, Turkey

Grund, M.: michael.grund@partner.kit.edu, Geophysical Institute (GPI), Karlsruhe Institute of Technology (KIT), Hertzstraße 16 Geb. 6.42, 76187 Karlsruhe, Germany

Mauerberger, A.: gassner@gfz-potsdam.de, GFZ-Potsdam, Albert-Einstein-Straße 42-46, Building A 46, 14473 Potsdam, Germany

Makushkina, A.: anya.makushkina@gmail.com, Research School of Earth Sciences, Australian National University, Canberra, ACT 0200, Australia

Artemieva, I.M.: iartemieva@gmail.com, GEOMAR Helmholtz Centre for Ocean Research Kiel, Wischhofstraße 1-3, 24148 Kiel, Tyskland, and Department of Geophysics, 397 Panama Mall, Mitchell Building, Stanford University, Stanford, CA 94305-2215, USA

Balling, N.: niels.balling@geo.au.dk, Department of Geoscience, Aarhus University, Høegh-Guldbergs Gade 2. DK-8000 Aarhus C, Denmark

Gudmundsson, O.: olafur.gudmundsson@geo.uu.se, Department of Earth Sciences, Uppsala University, Villavägen 16, 752 36 Uppsala, Sweden

Maupin, V.: valerie.maupin@geo.uio.no, Center for Earth Evolution and Dynamics (CEED), University of Oslo, Blindern, 0316 Oslo, Norway

Ottemøller, L.: lars.ottemoller@uib.no, Department of Earth Sciences, University of Bergen. Allegaten 41, 5007 Bergen, Norway

Ritter, J.: joachim.ritter@kit.edu, Geophysical Institute (GPI), Karlsruhe Institute of Technology (KIT), Hertzstraße 16, Geb. 6.42, 76187 Karlsruhe, Germany

Tilmann, F.: tilmann@gfz-potsdam.de, GFZ-Potsdam, Albert-Einstein-Straße 42-46, Building A 46, 14473 Potsdam, Germany

FIGURE CAPTIONS

Figure 1. a) Hypsometric map of the Baltic Shield and surrounding areas. The Northern (ND) and Southern (SD) Dome of the Scandes mountain range are indicated.

b) Tectonic sketch map of the Baltic Shield [after *Gaal and Gorbatschev, 1987]*. Full and dotted straight lines divide the southern (4), central (5) and northern (6) domains of the Svecofennian province.

Stippled line (black in a and yellow in b) shows location of profile illustrated in Figure 4. Encircled numbers refer to segments of the profile as explained by color code in the legend and the three Svecofennian domains.

Figure 2. a) Overview map of station locations in the Baltic Shield during temporary deployments. The ScanArray programme includes the ScanArray Core deployment 2012-2017 and the affiliated deployments shown in second box. Earlier deployments are illustrated in the following three boxes.

b) Seismic event distribution used for finite frequency tomography, cf. Figure 4f-h. Events in the first quadrangle are dominant, whereas only few events are observed from southerly directions.

Figure 3. Noise power spectral density probability density functions (PSDPDFs) plots for the vertical (left) and North-South components (right) of stations (from top to bottom) H2HS, SA20 and SA39. The plots are computed for one year of data (2014) with the IRIS System for Portable Assessment of Quality (ISPAQ version 2.0.0, provides the Modular Utility for STAtistical kNowledgeGathering [MUSTANG] data- quality metrics; Casey et al. 2018).

The gray curves are the New High and New Low Noise Model curves after Peterson (1993). The blue and red curves are the maximum and minimum measured noise levels, respectively.

Figure 4. Record sections for a) a local event in the Bothnian Bay on 2016/03/19 with magnitude 4.1, band-pass filtered between 0.04 and 2 Hz, and b) an event in Nepal on 2015/04/25 with magnitude 7.8, band-pass filtered between 0.01 and 0.5 Hz. Theoretical arrival times for all expected phases are highlighted in the sections.

Figure 5. Variation in topography and seismic properties along a NNE-SSW trending transect across the Baltic/Fennoscandian shield (a-j) as shown by stippled line in k).

a) Topography along the profile with abbreviations describing the tectonic segments, cf. Figure 1.
b) Crustal velocity structure obtained by surface wave tomography *(after Mauerberger et al., 2020).*
c) P-wave receiver functions.
d) S-wave receiver functions.
e) Mantle velocity structure obtained by surface wave tomography *(after Mauerberger et al., 2020).*
f) Mantle P-wave velocity structure obtained by finite frequency tomography.
g) Mantle S-wave velocity structure obtained by finite frequency tomography.
h) Mantle Vp/Vs ratio obtained by finite frequency tomography.
i) P-wave Receiver Functions for the mantle structure, showing constant depths to the ’410’ and ‘660’ discontinuities as well as possible strong converters in the 100-200 km depth range which, however, may be subject to severe interference from multiple arrivals (after *Makushkina et al., 2019*).

j) Variation in seismic anisotropy for selected permanent (white triangles) and temporary (gray triangles) recording stations in a 70 km wide corridor around the profile as obtained from shear-wave splitting (after *Grund and Ritter, 2020*). Splitting parameters (small bars, fast axis direction Φ and delay time δt) are shown in stereoplot-view as a function of backazimuth (BAZ, clockwise direction from North) and incidence angle (inc., radial axis). The orientation of Φ is additionally color-coded. Delay time δt scales with the length of the single bars. Null measurements (indicating no splitting) are shown as black open circles. The anisotropy shows distinct regional differences which appear correlated to tectonic provinces.

k) Hypsometric map of the study region. Stippled line shows location of profile illustrated in Figure 5. Encircled numbers refer to segments of the profile as given by colour code in the legend. Segments 4, 5 and 6 refer to subdivision of the Svecofennian province into its southern, central and northern domains. The Northern Dome (ND) appears to be located only within the Northern Svecofennian domain and the Southern Dome appears to be located solely within the Southern Svecofennian domain below segments that have been subject to later deformation during the Sveconorwegian and Caledonian orogenies, cf. Figure 1.

Figure 1

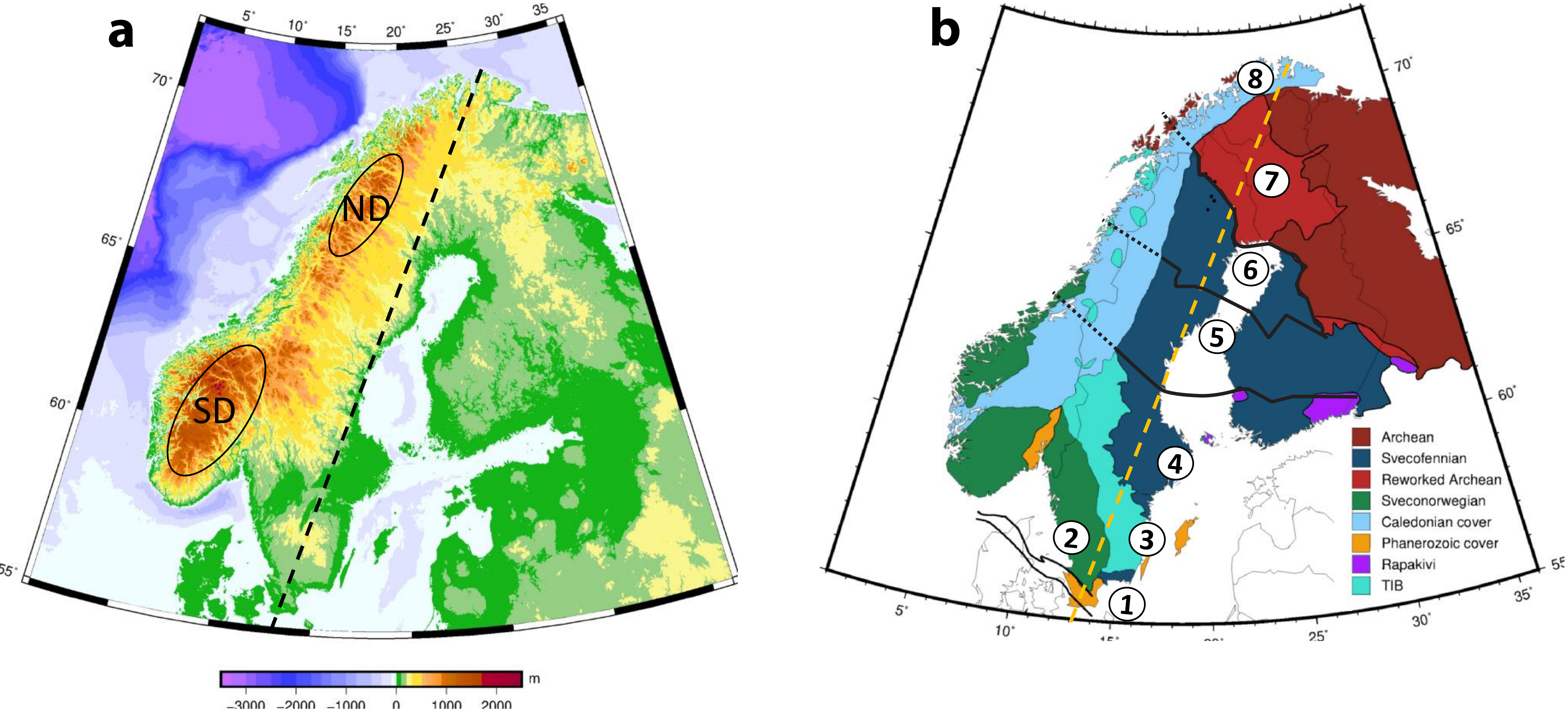
a
ND
SD
m
b
1
2
3
4
5
6
7
8
Archean
Svecofennian
Reworked Archean
Sveconorwegian
Caledonian cover
Phanerozoic cover
Rapakivi
TIB

Figure 2

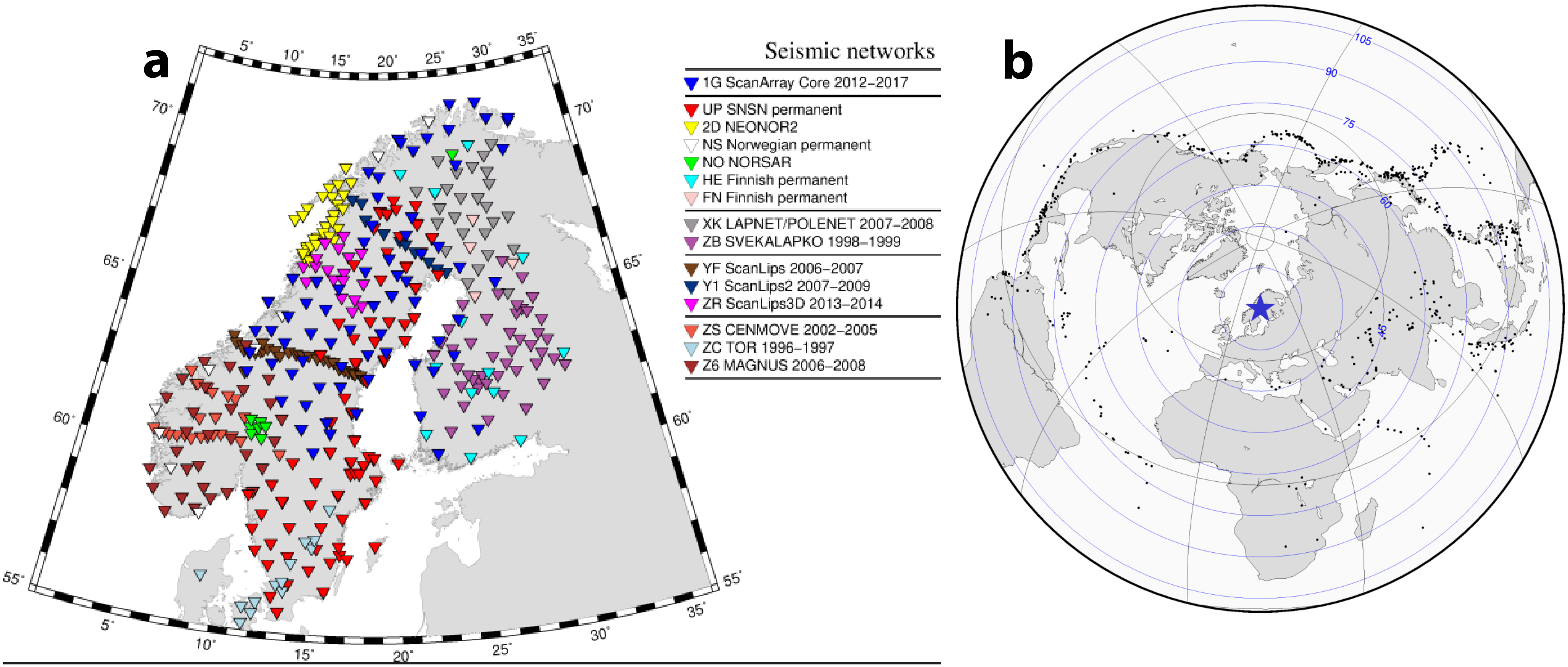
a
b
Seismic networks
1G ScanArray Core 2012–2017
UP SNSN permanent
2D NEONOR2
NS Norwegian permanent
NO NORSAR
HE Finnish permanent
FN Finnish permanent
XK LAPNET/POLENET 2007–2008
ZB SVEKALAPKO 1998–1999
YF ScanLips 2006–2007
Y1 ScanLips2 2007–2009
ZR ScanLips3D 2013–2014
ZS CENMOVE 2002–2005
ZC TOR 1996–1997
Z6 MAGNUS 2006–2008
105
90
75
60
45

Figure 5a-j

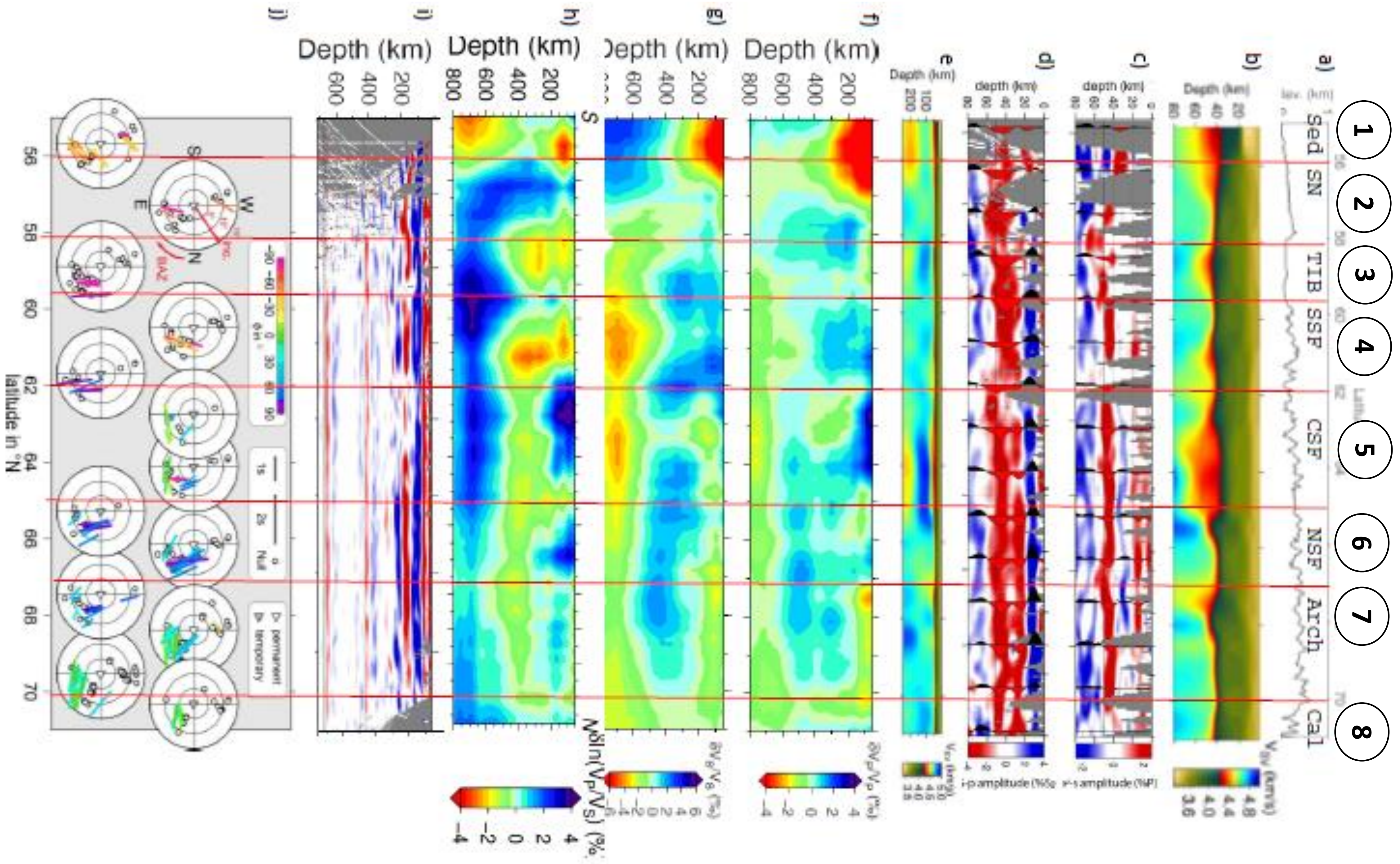

a)
b)
c)
d)
e
f)
g)
h)
i)
j)
1
2
3
4
5
6
7
8
Sed
SN
TIB
SSF
CSF
NSF
Arch
Cal
Depth (km)
latitude in °N

Figure 5k

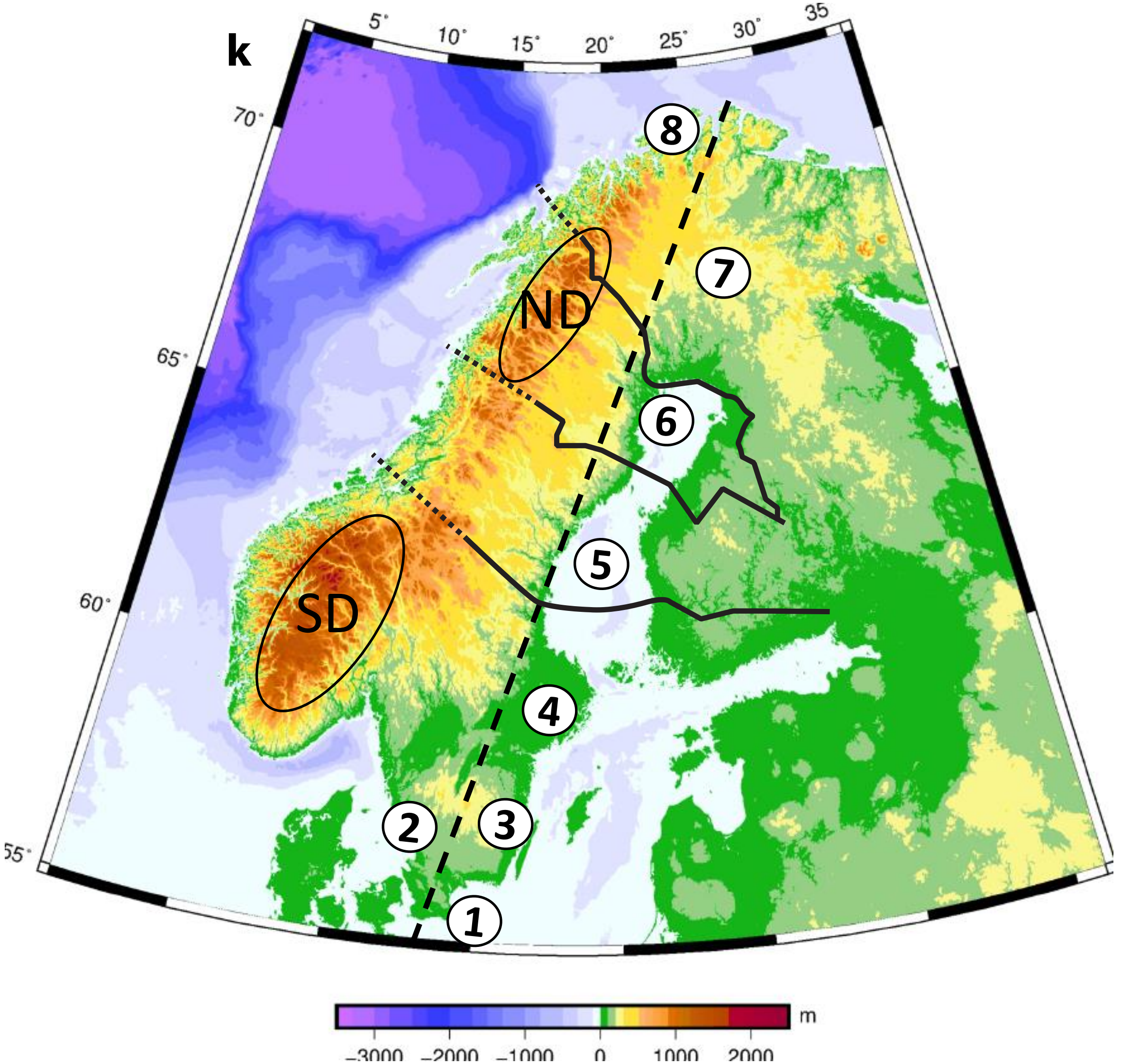

k
5°
10°
15°
20°
25°
30°
35
70°
65°
60°
55°
ND
SD
1
2
3
4
5
6
7
8
m
−3000
−2000
−1000
0
1000
2000

Figure 3

Click here to access/download;Figure;Figure 3.jpg

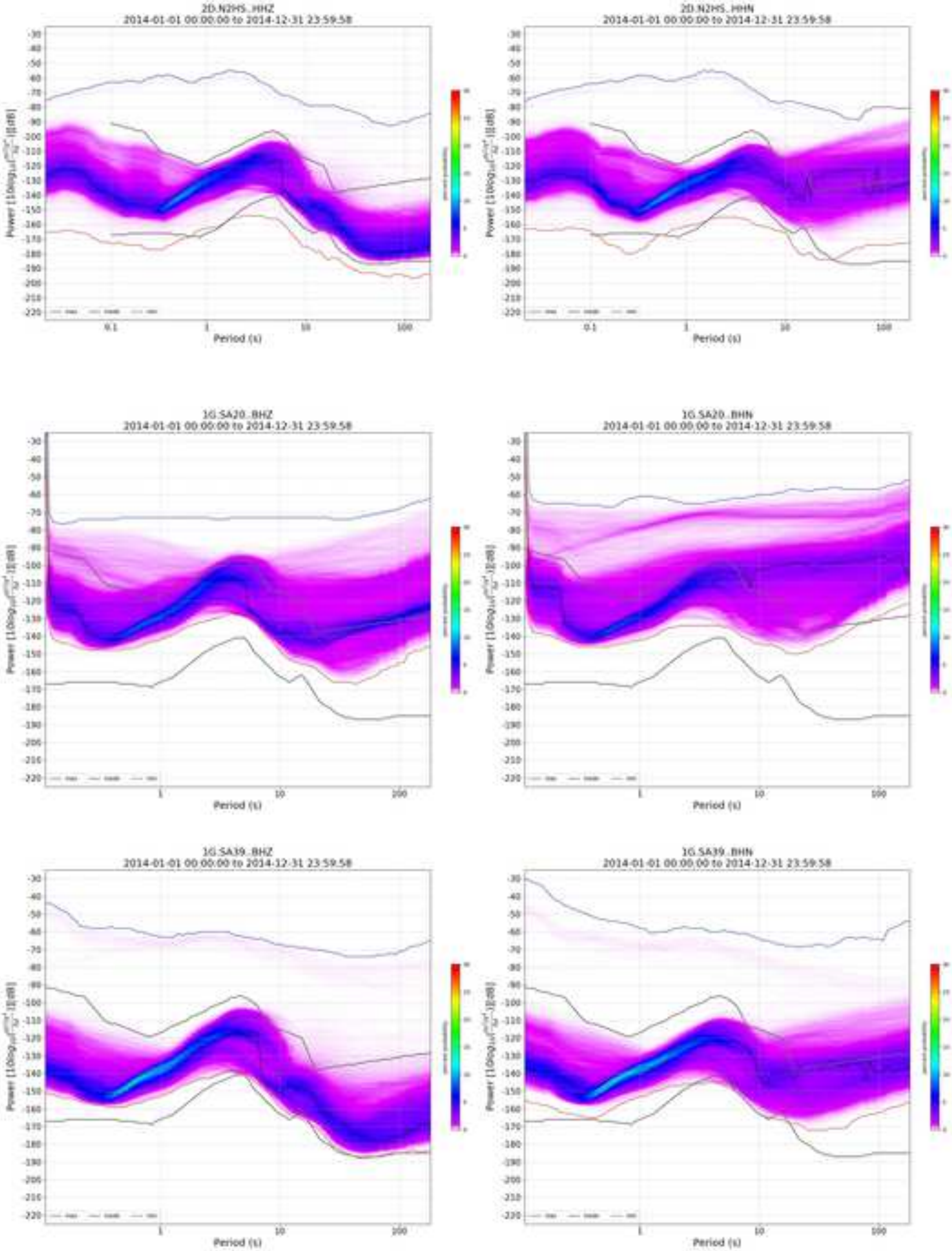

Figure 4a

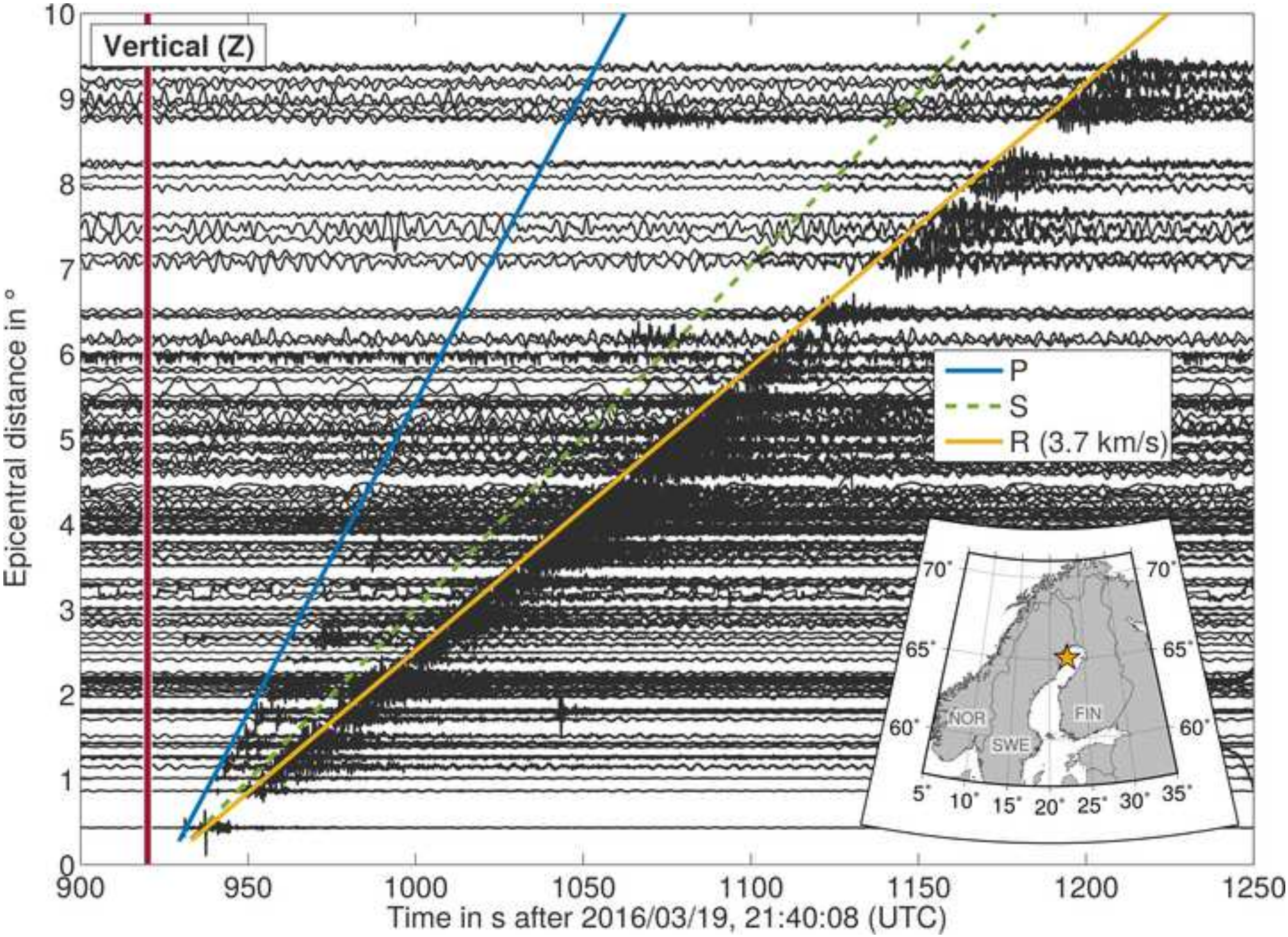
Vertical (Z)
P
S
R (3.7 km/s)
Epicentral distance in °
Time in s after 2016/03/19, 21:40:08 (UTC)
0
1
2
3
4
5
6
7
8
9
10
900
950
1000
1050
1100
1150
1200
1250
70°
65°
60°
5°
10°
15°
20°
25°
30°
35°
NOR
SWE
FIN

Figure 4b

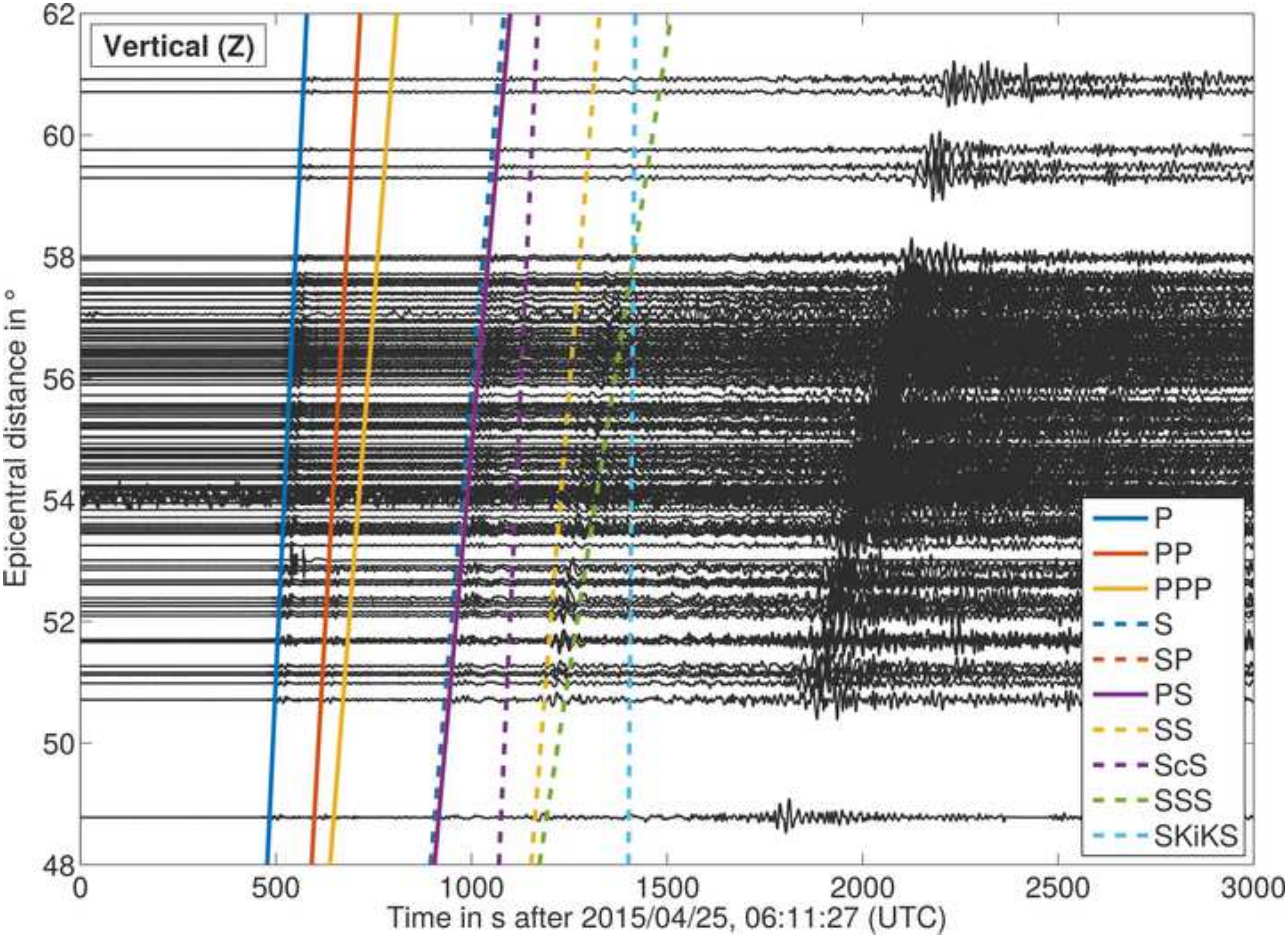

Vertical (Z)
62
60
58
56
54
52
50
48
Epicentral distance in °
0
500
1000
1500
2000
2500
3000
Time in s after 2015/04/25, 06:11:27 (UTC)
P
PP
PPP
S
SP
PS
SS
ScS
SSS
SKiKS

Supplementary Material to

ScanArray – A broad band seismological experiment in the Baltic Shield

by H. Thybo et al.

Submitted to Seismological Research Letters on 12 January 2021

Figure S1. Maps illustrating the temporal evolution of the ScanArray deployment in relation to other broad band seismological deployments in Fennoscandia. a) Stations in summer 2012, b) Stations in summer 2013, c) Stations in summer 2014, d) Stations in spring 2015, e) Earlier deployments, f) Total coverage of Fennoscandia at end of the ScanArray deployment.

Table S1. List of stations in the ScanArray 1G core station deployment with operating institution coded in column "Operator". Period refers to seismometer period. Operational refers to the number of years each station was deployed.

Summer 2012

Figure S1a

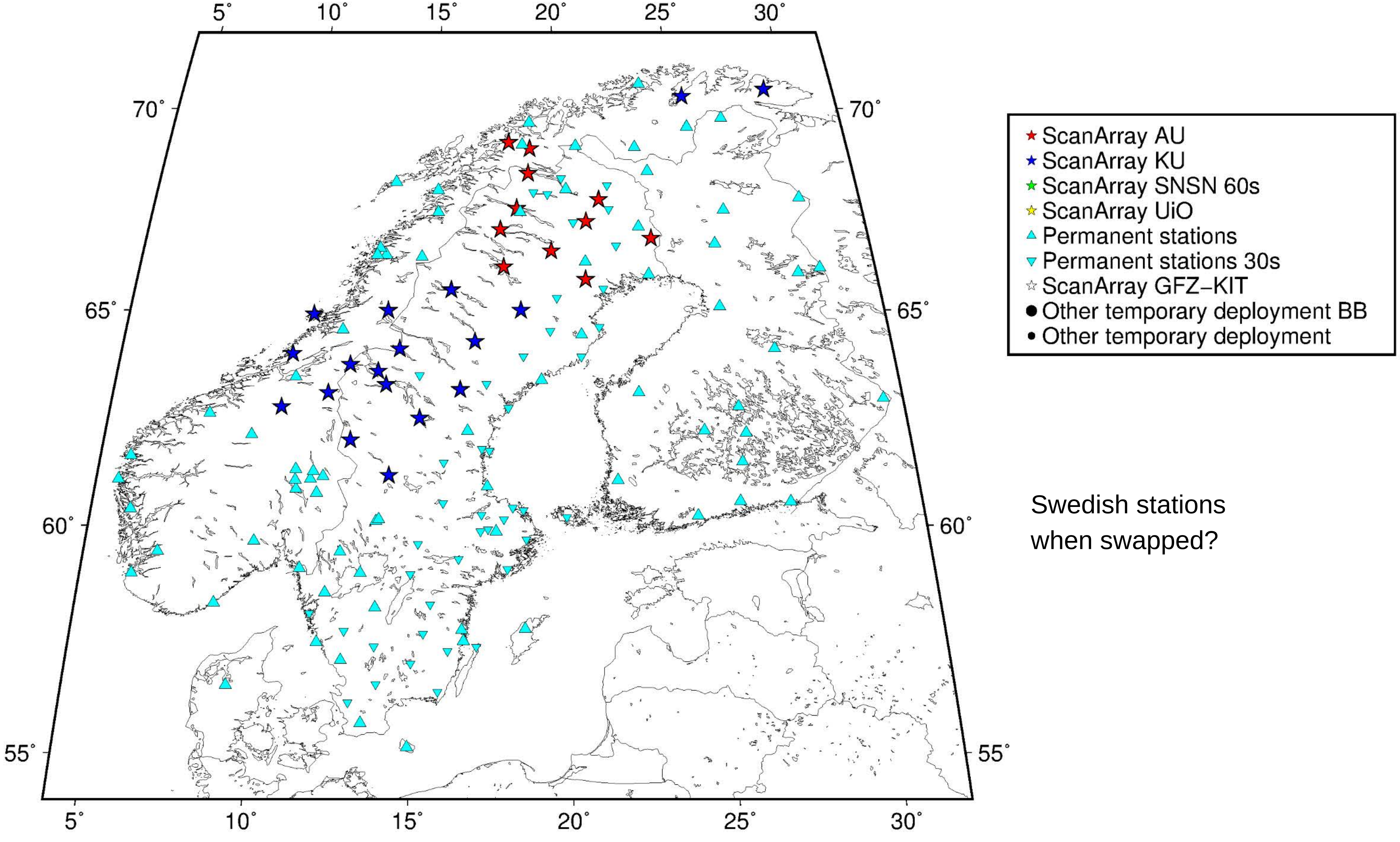

Swedish stations when swapped?

Summer 2013

Figure S1b

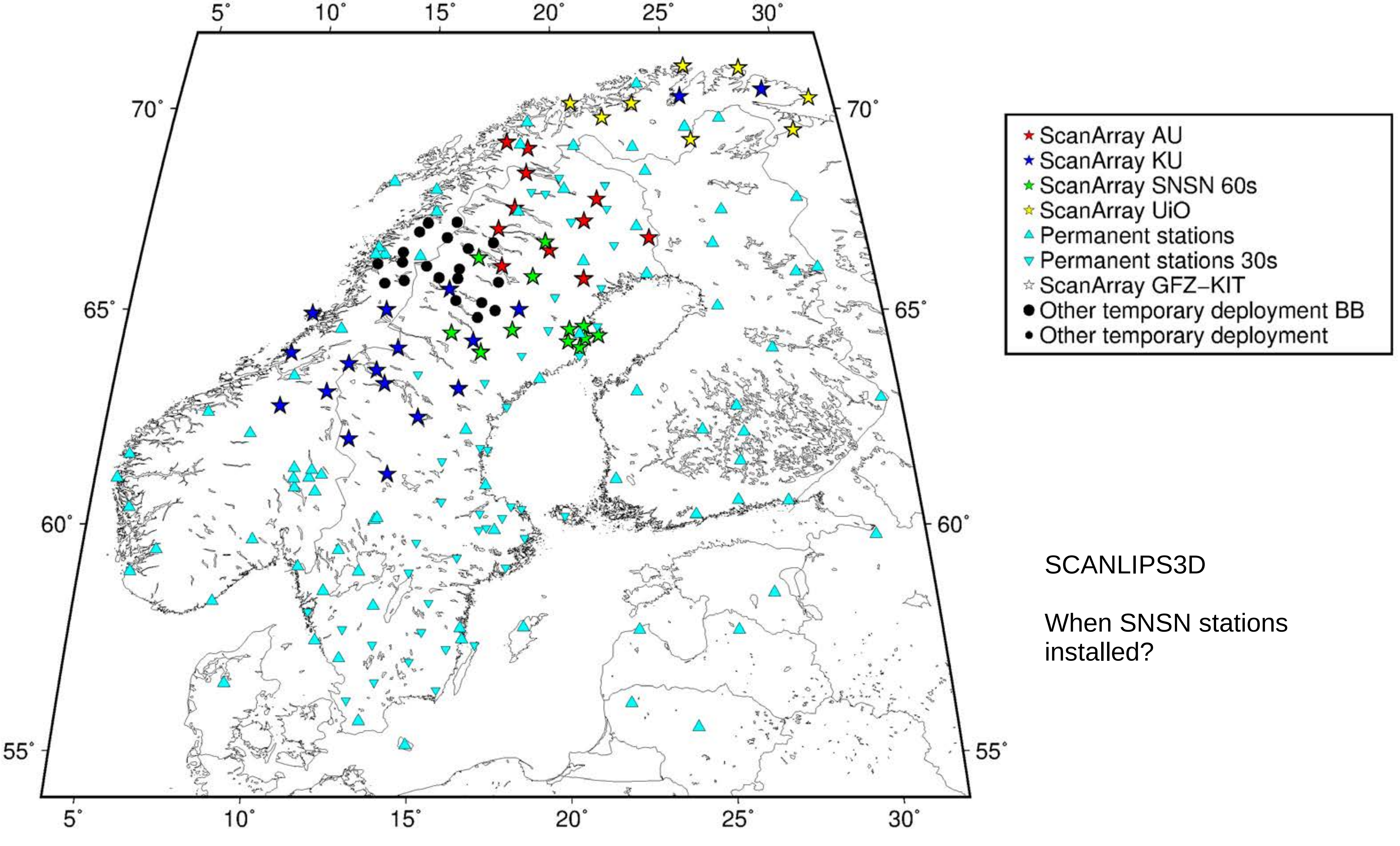

SCANLIPS3D

When SNSN stations installed?

Summer 2014

Figure S1c

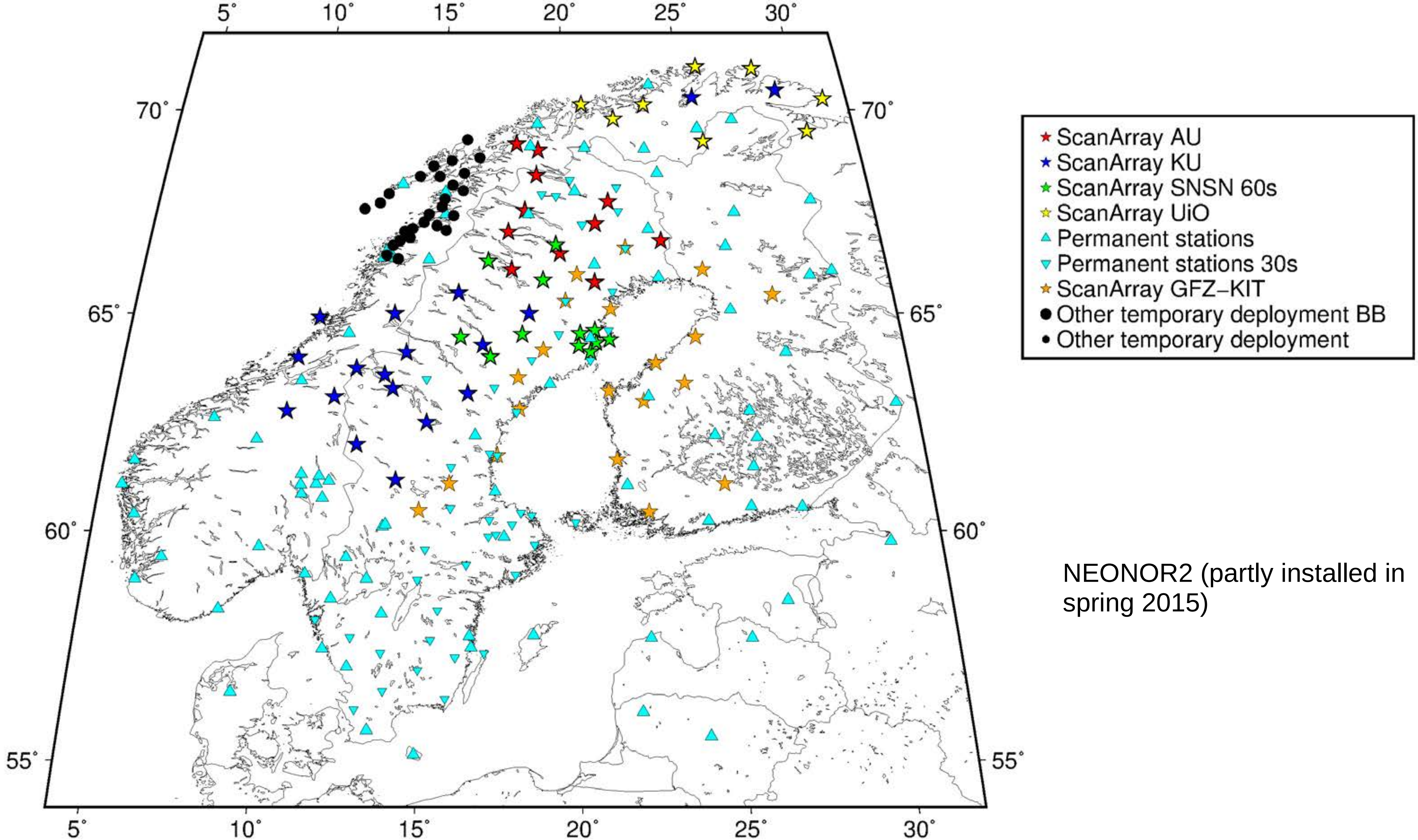

NEONOR2 (partly installed in spring 2015)

Spring 2015

Figure S1d

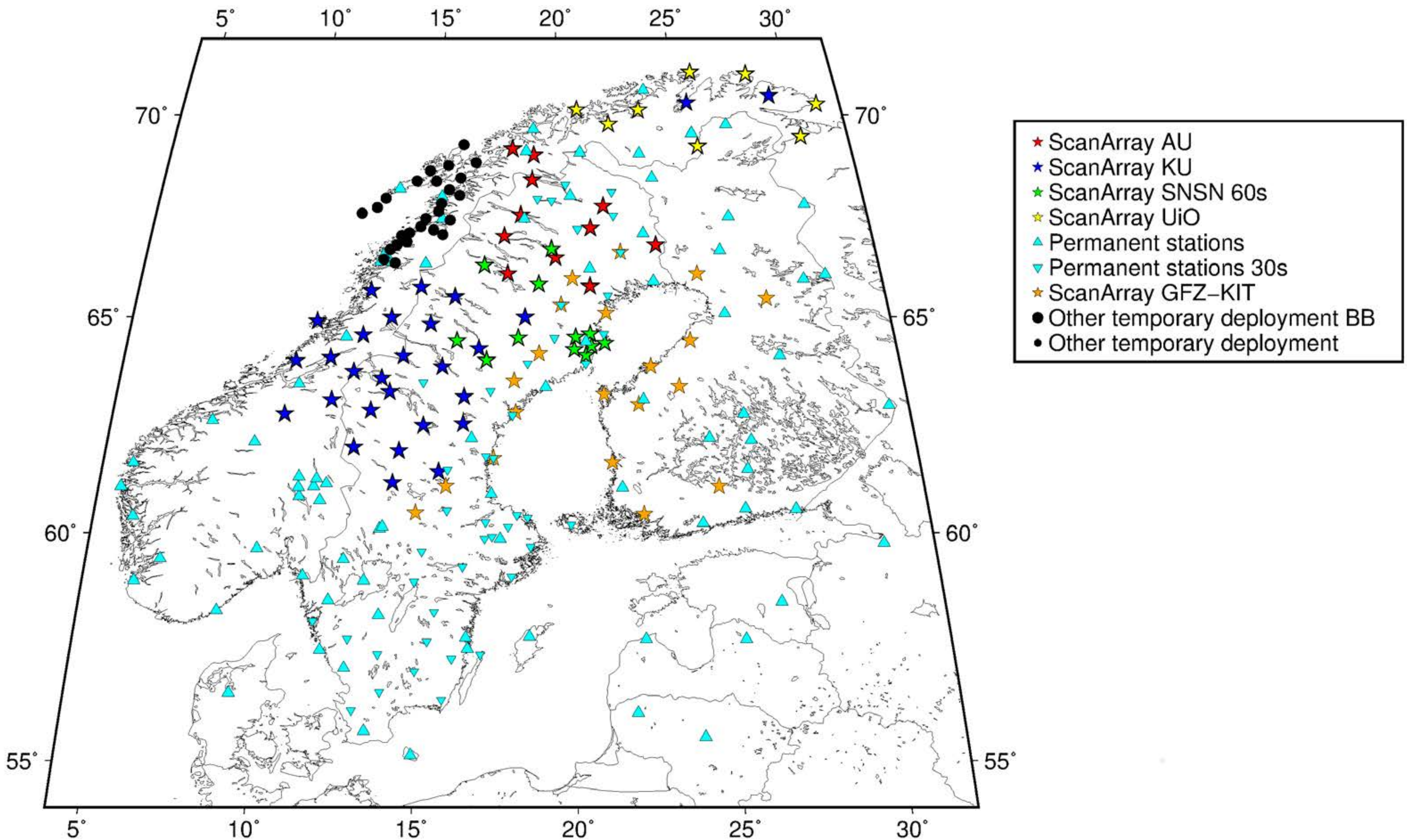

Earlier deployments

Figure S1e

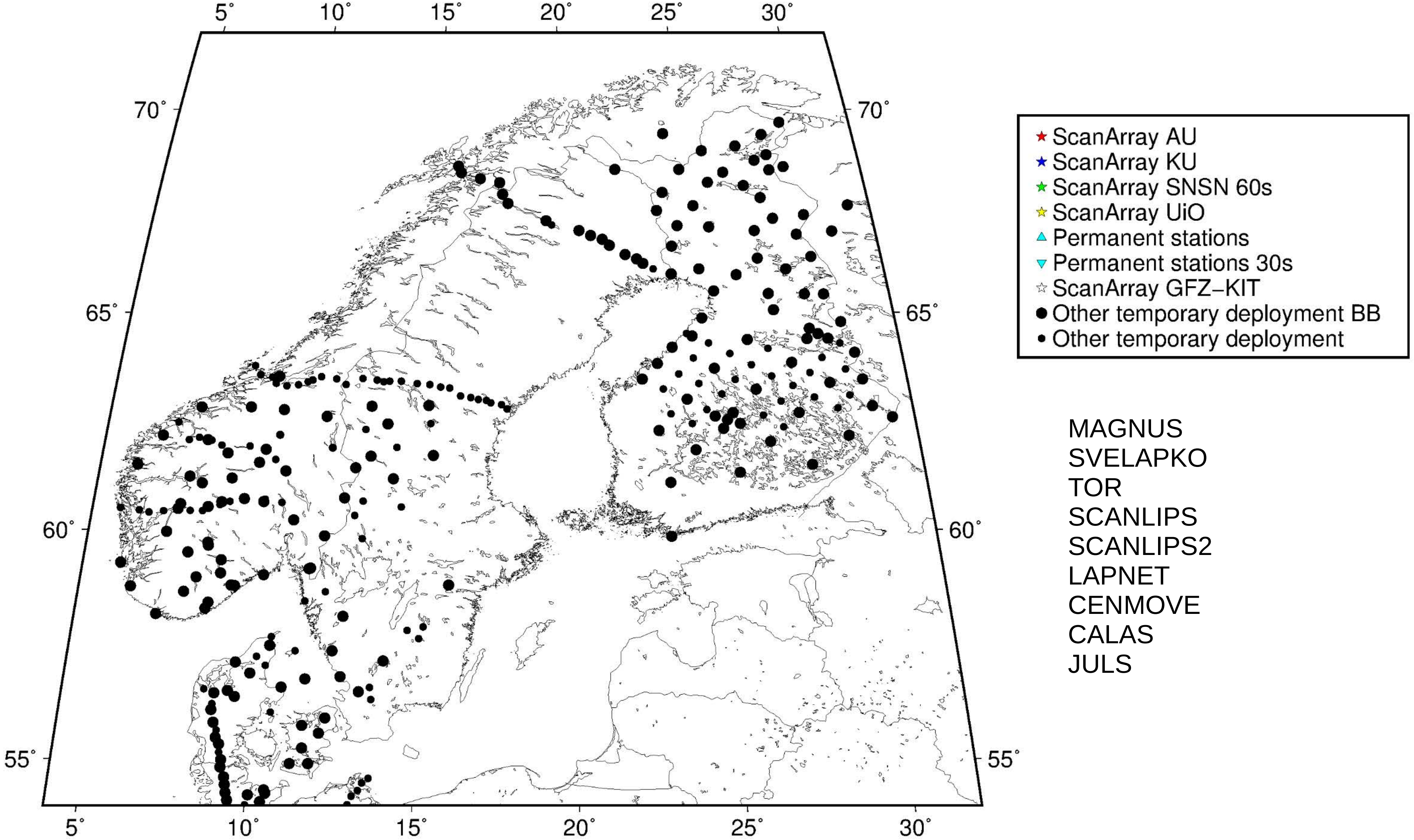

MAGNUS
SVELAPKO
TOR
SCANLIPS
SCANLIPS2
LAPNET
CENMOVE
CALAS
JULS

Total coverage of Fennoscandia

Figure S1f

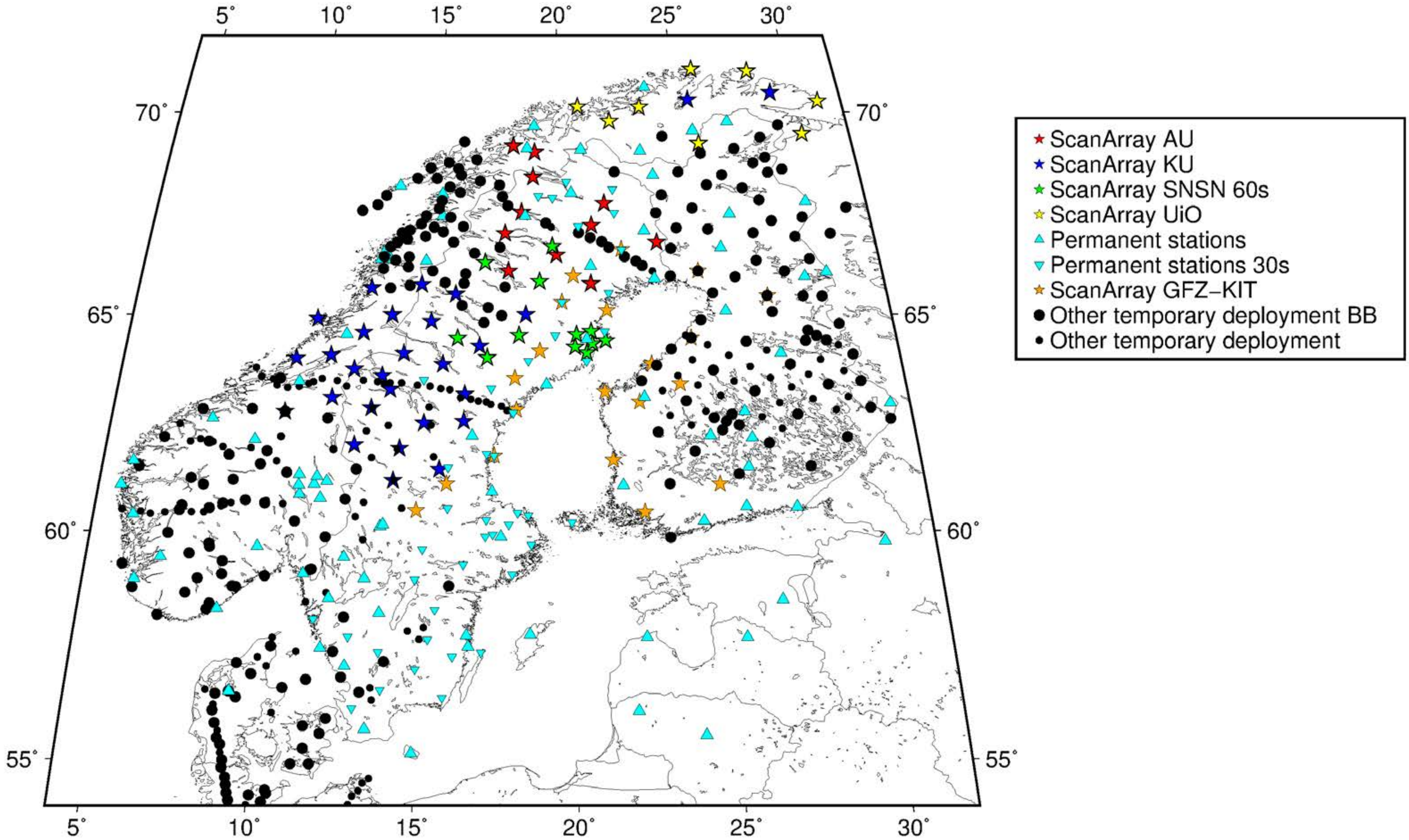

Table S1. List of stations in the ScanArray 1G core station deployment with operating institution coded in column "Operator". Period refers to seismometer period. Operational refers to the number of years each station was deployed.

Station	Operator	Latitude (°N)	Longitude (°E)	Elevation (m)	Period (s)	Deployed	Operational (y)
SA01	UiO	71.11106	25.81695	14	120	26/09/2013	3
SA02	UiO	71.06376	28.24166	13	120	25/09/2013	3
SA03	KU	70.50340	29.06682	272	120	03/08/2012	5
SA04	KU	70.31915	25.47692	71	120	31/07/2012	5
SA05	UiO	70.28404	31.00829	33	120	24/09/2013	3
SA06	UiO	70.13431	20.75993	5	120	27/09/2013	3
SA07	UiO	70.12715	23.37370	18	120	26/09/2013	3
SA08	UiO	69.76423	22.06233	13	120	28/09/2013	3
SA09	UiO	69.45361	30.03907	28	120	23/09/2013	3
SA10	UiO	69.20068	25.69157	155	120	25/09/2013	3
SA11	AU	69.13213	18.04955	6	120	06/09/2012	4
SA12	AU	68.97312	18.91437	39	120	07/09/2012	4
SA13	AU	68.34912	18.83685	382	120	06/09/2012	4
SA14	AU	67.69623	21.62417	248	120	05/09/2012	4
SA15	AU	67.47458	18.36473	383	120	08/09/2012	4
SA16	AU	67.15173	21.07752	334	120	05/09/2012	4
SA17	AU	66.95288	17.72637	335	120	09/09/2012	4
SA18	AU	66.73932	23.56422	173	120	04/09/2012	4
SA19	GFZ+KIT	66.56536	22.17883	98	120	18/09/2014	2
SA20	AU	66.42983	19.68620	380	120	09/09/2012	4
SA21	GFZ+KIT	66.04059	25.03044	70	120	01/10/2014	2
SA22	AU	66.03818	17.85910	498	120	10/09/2012	4
SA23	GFZ+KIT	65.92625	20.30078	117	120	20/09/2014	2
SA24	AU	65.73557	20.95423	58	120	10/09/2012	4
SA25	KU	65.67228	14.22488	476	240	01/03/2015	2
SA26	KU	65.69917	12.43827	0	240	03/2015	2
SA27	KU	65.48233	15.89654	444	120	09/2012	5

SA28	GFZ+KIT	65.44692	27.52064	160	120	01/10/2014	2
SA29	GFZ+KIT	65.28787	19.84522	335	240	21/09/2014	2
SA30	GFZ+KIT	65.09228	21.49773	6	120	21/09/2014	2
SA31	KU	64.99111	18.50105	271	120	09/2012	5
SA32	KU	64.98758	13.58130	478	120	09/2012	5
SA33	KU	64.90327	10.84991	9	120	09/2012	5
SA34	KU	64.83179	15.03127	537	240	03/2015	2
SA35	KU	64.53397	12.40071	123	240	03/2015	2
SA36	GFZ+KIT	64.44019	24.51723	50	120	01/10/2014	2
SA37	KU	64.24671	16.81777	414	120	09/2012	5
SA38	GFZ+KIT	64.12913	19.00028	236	120	16/09/2014	2
SA39	KU	64.07180	14.09061	351	120	09/2012	5
SA40	KU	64.04353	11.33531	45	240	03/2015	2
SA41	KU	63.96652	10.23171	18	120	09/2012	5
SA42	GFZ+KIT	63.82646	23.00790	10	120	10-2014	2
SA43	KU	63.81655	15.51477	333	240	03/2015	2
SA44	KU	63.70518	12.34839	462	120	09/2012	5
SA45	KU	63.54918	13.36576	413	120	09/2012	5
SA46	GFZ+KIT	63.48963	18.09452	140	120	15/09/2014	2
SA47	GFZ+KIT	63.35959	23.97327	100	120	01/10/2014	2
SA48	KU	63.23047	13.67801	401	120	09/2012	5
SA49	GFZ+KIT	63.17494	21.27882	40	120	01/10/2014	2
SA50	KU	63.11401	16.32236	153	120	09/2012	5
SA51	KU	63.04408	11.64370	474	120	09/2012	5
SA52	GFZ+KIT	62.93811	22.48778	40	240	01/10/2014	2
SA53	KU	62.80045	13.05265	568	240	03/2015	2
SA54	GFZ+KIT	62.75039	18.14890	13	240	14/09/2014	2
SA55	KU	62.71911	10.03964	533	120	09/2012	5
SA56	KU	62.48589	16.30865	84	240	03/2015	2
SA57	KU	62.44944	14.92132	271	120	09/2012	5
SA58	KU	61.94490	12.55341	562	120	09/2012	5

SA59	KU	61.86536	14.12029	481	240	03/2015	2
SA60	GFZ+KIT	61.69295	17.37935	15	120	13/09/2014	2
SA61	GFZ+KIT	61.59337	21.46223	10	120	01/10/2014	2
SA62	KU	61.38391	15.51161	204	240	03/2015	2
SA63	KU	61.13399	13.95659	449	120	09/2012	5
SA64	GFZ+KIT	61.05372	25.03989	130	240	01/10/2014	2
SA65	GFZ+KIT	61.05349	15.76985	99	120	12/09/2014	2
SA66	GFZ+KIT	60.44683	14.78057	239	120	2014-09-11	2
SA67	GFZ+KIT	60.41585	22.44386	50	120	01/10/2014	2

Operator abbreviations:

AU: Aarhus University

GFZ+KIT: Geoforschungszentrum Potsdam and Karlsruhe Institute of Technology

KU: University of Copenhagen

UiO: University of Oslo